ABSTRACT

CHARACTERIZATION OF LOW PRESSURE CHEMICALLY VAPOR DEPOSITED BORON NITRIDE FILMS AS LOW DIELECTRIC CONSTANT MATERIALS

by
Manish Narayan

Boron nitride thin films were synthesized on Si and quartz wafers by low pressure chemical vapor deposition using borane triethylamine complex and ammonia as precursors. The films were processed at 400°C, 475°C and 550°C at a constant pressure of 0.5 Torr and at different precursor flow ratios.

The films deposited were uniform, amorphous and the composition of the films varied with deposition temperature and precursor flow ratios. The thickness of the film increased with increasing flow ratio, but, decreased with increasing temperature. The stresses in the film were either mildly tensile or compressive.

The least dielectric constant for the films that could be attained was 2.73 at 550°C and at high flow ratios of NH_3/TEAB (50/1). Thus, stoichiometric boron nitride films tend to have a lower dielectric constant. The limitation of attaining lower values could be due to the presence of carbon as an impurity in the film and the presence of mobile charge carriers in the films as well as at the substrate-film interface as seen from the capacitance-voltage characteristics.

CHARACTERIZATION OF LOW PRESSURE CHEMICALLY VAPOR DEPOSITED BORON NITRIDE FILMS AS LOW DIELECTRIC CONSTANT MATERIALS

by
Manish Narayan

A Thesis
Submitted to the Faculty of
New Jersey Institute of Technology
in Partial Fulfillment of the Requirements for the Degree of
Master of Science in Engineering Science

Interdisciplinary Program in Materials Science and Engineering

January 1996

APPROVAL PAGE

CHARACTERIZATION OF LOW PRESSURE CHEMICALLY VAPOR DEPOSITED BORON NITRIDE FILMS AS LOW DIELECTRIC CONSTANT MATERIALS

Manish Narayan

Dr. Roland A. Levy, Thesis Advisor — Date
Professor of Physics,
Director of Materials Science and Engineering Program, NJIT

Dr. Lev N. Krasnoperov, — Date
Professor of Chemical Engineering, Chemistry, and
Environmental Science, NJIT

Dr. N.M. Ravindra, — Date
Professor of Physics,
Associate Director, Electronic Imaging Center, NJIT

BIOGRAPHICAL SKETCH

Author: Manish Narayan

Degree: Master of Science in Engineering Science

Date: January, 1996

Date of Birth:

Place of Birth:

Undergraduate and Graduate Education:

- Master of Science in Engineering Science,
  New Jersey Institute of Technology,
  Newark, New Jersey, 1996

- Master of Engineering in Metallurgy,
  Indian Institute of Science,
  Bangalore, India, 1993

- Bachelor of Science in Physics, Chemistry and Mathematics,
  Bangalore University,
  Bangalore, India, 1989

Major: Materials Science and Engineering

Professional Experience

Research Assistant	CVD Laboratory, NJIT	1995-96
Production Engineer	Titan Industries Ltd. Jewelry Div., Bangalore, India	1993-95
Project Assistant	Indian Institute of Science, Bangalore, India	1992-93

This thesis is dedicated to
my parents

ACKNOWLEDGMENT

The author express his sincere gratitude to his advisor, Professor Roland A. Levy for his guidance, inspiration, and support throughout this research.

Special thanks to Professor N.M. Ravindra and Professor Lev N. Krasnoperov for serving as members of the thesis review committee.

The author his gratitude to Dr. Zia Karim of Sharp Microelectronics Inc. for performing the electrical characterization of the samples.

The author appreciates the timely help and suggestions from Dr. Jan Opyrchal and Emmanuel Ramos and other CVD laboratory members including, Vitaly Sigal, Romiana Petrova, Venkat Paturi, Mahalingam Bhaskaran, Chenna Ravindranath, David Perese, Kiran V Chatty and Majda Newman.

TABLE OF CONTENTS

TABLE OF CONTENTS
(Continued)

Chapter **Page**

TABLE OF CONTENTS
(Continued)

Chapter **Page**

LIST OF TABLES

LIST OF FIGURES

Figure **Page**

LIST OF FIGURES
(Continued)

CHAPTER 1

INTRODUCTION

Boron nitride is one of the most interesting materials of the III-V compounds, from both the theoretical as well as the application viewpoint. The useful properties of boron nitride such as its low density, high thermal conductivity, chemical inertness, high hardness, low dielectric constant and high resistivity find wide range of industrial applications.

Extensive work has been done to synthesize this material in the form of thin films due to its technological importance in many areas. Boron nitride thin films can form transparent insulating thin films which combine extreme hardness with resistance to oxidation at high temperatures. These films can protect working metal parts from corrosion and wear. Earlier investigations have reported some favorable properties of amorphous BN films for the fabrication of X-ray mask membranes and for the use as a intermetal dielectric material with low dielectric constant. The latter becomes extremely important with miniaturization of electronic circuits with increased complexity and multilevel metal layers.

Dielectric materials are widely used in capacitors which store electric charge. Under the influence of an electric field, the electrons freely move through conductors, whereas in dielectrics, the charges are separated slightly from their normal positions, polarizing the material. When the dielectric is placed between the plates of a capacitor, the capacitance or the ability to store charge is increased by a factor equal to the dielectric constant. The dielectric constant of the material is dependent on the extent of permanent polarized bonding and the angles between chemical bonds. The less polarizable dielectric materials will have a lower dielectric constant.

The most desired intermetal dielectric material that can be used in advanced high density semiconductor devices should have a low dielectric constant, low mechanical stress, high thermal stability (>450°C) and low moisture absorption. Aluminum interconnected with silicon oxide as intermetal dielectric is used presently results in high parasitic capacitance and cross talk interference in high density devices.

Apart from silicon oxide one of the most promising intermetal dielectric material that provides reduction in dielectric constant is boron nitride. Hence the primary aim of the present work is to

- fabricate boron nitride thin films
- characterize these films
- optimize deposition parameters to obtain low stress and low dielectric constant films.

Chemical vapor deposition is one of the methods of fabricating boron nitride thin films. The process and the salient features of the process are described in the subsequent sections. Further, the properties of dielectric materials and their applications in very large scale integrated (VLSI) technology is discussed.

In Chapter 2, a review of literature of boron nitride thin films; the preparation techniques, their properties are discussed. In addition, an overview of low dielectric constant materials in general, and BN and SiBN thin films as low dielectric constant materials in particular, are discussed.

In Chapter 3, the experimental procedure to fabricate boron nitride films and the characterization techniques used are described.

The important results of this work are described in Chapter 4 and the effect of various deposition parameters on the properties are discussed in detail.

Concluding remarks and suggestions for future work are given in Chapter 5.

1.1 Chemical Vapor Deposition

Chemical Vapor Deposition (CVD) is one of the most important methods of film formation used in the fabrication of very large scale integrated (VLSI) silicon circuits, as well as of microelectronic solid state devices in general. In this process, chemicals in the gas or vapor phase are reacted at the surface of the substrate where they form a solid product. A large variety of materials, practically all those needed in microelectronic device technology, can be created by CVD. These materials comprise insulators and dielectrics, elemental and compound semiconductors, electrical conductors, superconductors and magnetics. In addition to its unique versatility, this materials synthesis and vapor phase growth method can operate efficiently at relatively low temperatures. For example, refractory oxide glasses and metals can be deposited at temperatures of only 300° to 500°C. This feature is very important in advanced VLSI devices with short channel lengths and shallow junctions, where lateral and vertical diffusion of the dopants must be minimized. This also helps in minimizing process-induced crystallographic damage, wafer warpage and contamination by diffusion of impurities.

1.1.1 Fundamental Aspects of CVD

Chemical vapor deposition is defined as a process whereby constituents of the gas or vapor phase react chemically near or on the substrate surface to form a solid product. This product can be in the form of a thin film, a thick coating, or if allowed to grow, a massive bulk. It can have a single-crystalline, poly-crystalline, or amorphous structure. Chemical and physical conditions during the deposition reaction can strongly affect the composition and structure of the product. This deposition technology has become one of the most means of creating thin films and coatings in solid state microelectronics where some of the most sophisticated purity and composition requirements must be met.

Chemical reaction type basic to CVD include pyrolysis, oxidation, reduction, hydrolysis, nitride and carbide formation, synthesis reactions and chemical transport. A sequence of several reaction types may be involved to create a particular end product. The chemical reactions may take place not only on the substrate surface (heterogeneous reaction), but also in the gas phase (homogeneous reaction). Heterogeneous reactions are much more desirable, as such reactions selectively occur only on the heated surfaces, and produce good quality films. Homogeneous reactions, on the other hand are undesirable, as they form gas phase clusters of the depositing material, which will result in poor adherence, low density or defects in the film. Thus one important characteristic of CVD application is the degree to which heterogeneous reactions are favored over homogeneous reactions. This film could be a thin film or a thick coating and should be less volatile to remain on the substrate.

1.1.2 Transport Phenomena of CVD

CVD of the film is almost always a heterogeneous reaction. The sequence of the steps in the usual heterogeneous processes can be described as follows:

1. Arrival of the reactants
   a. bulk transport of reactants into the chamber,
   b. gaseous diffusion of reactants to the substrate surface,
   c. adsorption of reactants onto the substrate surface.
2. Surface chemistry
   a. surface diffusion of reactants,
   b. surface reaction.
3. Removal of by-products
   a. desorption of by-products from the substrate surface,
   b. gaseous diffusion of by-products away from the substrate surface,
   c. bulk transport of by-products out of the reaction chamber.

The steps are sequential and the slowest process is the rate determining step.

The sequential steps of deposition process can be grouped into (i) mass transport-limited regime and (ii) surface-reaction-limited regime. If the deposition process is limited by the mass transfer, the transport process occurred by the gas-phase diffusion is proportional to the diffusivity of the gas and the concentration gradient. The mass transport process which limits the growth rate is only weakly dependent on temperature. On the other hand, it is very important that the same concentration of reactants be present in the bulk gas regions adjacent to all locations of a wafer, as the arrival rate is directly proportional to the concentration in the bulk gas. Thus, to ensure films of uniform thickness, reactors which are operated in the mass-transport-limited regime must be designed so that all locations of wafer surfaces and all wafers in a run are supplied with an equal flux of reactant species.

If the deposition process is limited by the surface reaction, the growth rate, R, of the film deposited can be expressed as $R = R_o * \exp(-E_a/RT)$, where R_o is the frequency factor, E_a is the activation energy - usually 25-100 kcal/mole for surface process, R is the gas constant, and T, the absolute temperature. In the operating regime, the deposition rate is a strong function of the temperature and an excellent temperature control is required to achieve the film thickness uniformity that is necessary for controllable integrated circuit fabrication.

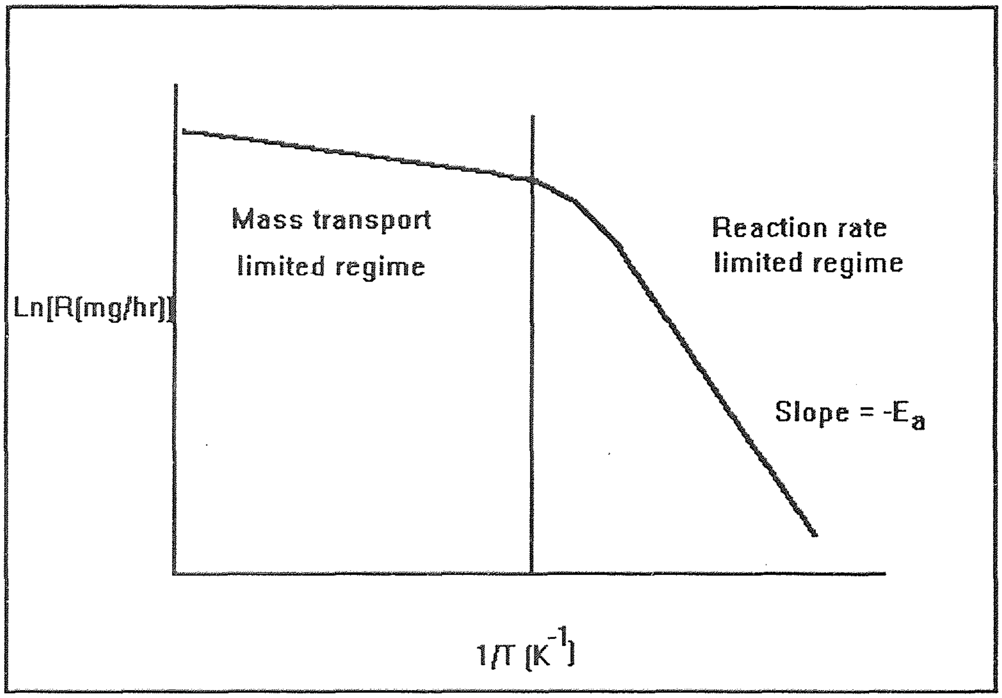

Figure 1.1 Deposition rate as a function of substrate temperature exemplifying diffusion controlled and surface-reaction controlled regimes

On the other hand, under such conditions the rate at which reactant species arrive at the surface is not as important. Thus, it is not as critical that the reactor be designed to supply an equal flux of reactants to all locations of the wafer surface. It will be seen that in horizontal low pressure CVD reactors, wafers can be stacked vertically and at very close spacing because such systems operate in a surface-reaction-rate limited regime. In deposition processes that are mass-transport limited, however, the temperature control is not nearly as critical. As shown in Figure 1.1, a relatively steep temperature range, and a milder dependence in the upper range, indicating that the nature of the rate-controlling step changes with temperature.

1.1.3 Film Growth Aspects of CVD

In general, lower temperature and higher gas phase concentration favor formation of polycrystalline deposits. Under these conditions, the arrival rate at the surface is high, but the surface mobility of adsorbed atoms is low. Many nuclei of different orientation are formed, which upon coalescence result in a film consisting of many differently oriented grains. Further decrease in temperature and increase in supersaturation result in even more nuclei, and consequently in finer-grained films, eventually leading to the formation of amorphous films when crystallization is completely prevented. Amorphous films include oxides, nitrides, carbides and glasses are of great technical importance for microelectronics applications.

Deposition variables such as temperature, pressure, input concentrations, gas flow rates, reactor geometry and reactor opening principle determine the deposition rate and the properties of the film deposit.

1.2 Low Pressure CVD Process

The most important and widely used CVD processes are atmospheric pressure CVD (APCVD), low pressure CVD (LPCVD) and plasma enhanced CVD (PECVD). Only LPCVD is discussed in detail below as this process is employed in this study.

Most low pressure CVD processes are conducted by resistance heating and less frequently infrared radiation heating techniques to attain isothermal conditions so that the substrate and the reactor walls are of similar temperature. The deposition rate and uniformity of the films created by all CVD processes are governed by two basic parameters (i) the rate of mass transfer of reactant gases to the substrate surface and (ii) the rate of surface reaction of the reactant gases at the substrate surface. Lowering the pressure to below atmospheric pressure enhances the mass transfer rate relative to the surface reaction rate thus making it possible to deposit films uniformly in a highly economical close spaced positioning of the substrate wafers in the standup position.

1.2.1 Mechanism

The mass transfer of the gases involve their diffusion across a slowly moving boundary layer adjacent to the substrate surface. The thinner this boundary layer and the higher the gas diffusion rate, the greater is the mass transport that results. Surface reaction rates, on the other hand, depend mainly upon reactant concentration and deposition temperature. High deposition rates are attainable with LPCVD despite the fact that the operating total pressure is usually two to four orders of magnitude lower than atmospheric CVD. This is due to the fact that the large mole fraction of reactive gases in LPCVD, and no or little diluent gas is required. Wafer spacing has a marked effect on the deposition rate of all types of films, the deposition rate increasing linearly with increasing spacing since the quantity of available reactant per wafer increases.

1.2.2 Factors Affecting Film Uniformity

Some of the main factors affecting the film thickness uniformity in LPCVD are the temperature profile in the reactor, the pressure level in the reactor and the reactant gas flow rates. To obtain a flat thickness profile across each substrate wafer throughout the reactor requires a judicious adjustments of these parameters. In tubular reactors, increase in temperature or pressure, increases the deposition rate upstream, thereby using up more reactant gases and leaving less to react at the downstream end; the opposite effect takes place on lowering the temperature and pressure. Similar effects occur with variations of the reactant gas flow rates at constant gas partial pressure, or with changes in the size and number of the wafers processed per deposition run. The uniformity of thickness and step coverage of these films are very good. These films have fewer defects, such as particulate contaminants and pinholes, because of their inherently cleaner hot wall operations and the vertical wafer positioning that minimize the formation and codeposition of homogeneously gas phase nucleated particulates.

1.3 Advantages of CVD

Thin films are used in a host of applications in VLSI fabrication, and can be synthesized by a variety of techniques. Regardless of the method by which they are formed, however, the process must be economical, and the resultant films must exhibit uniform thickness, high purity and density, controllable composition and stoichiometries, high degree of structural perfection, excellent adhesion and good step coverage. CVD processes are often selected over competing deposition techniques because they offer the following advantages:

1. A variety of stoichiometric and non stoichiometric compositions can be deposited by accurate control of process parameters.
2. High purity films can be deposited that are free from radiation damage without further processing.
3. Results are reproducible.
4. Uniform thickness' can be achieved by low pressures.
5. Conformal step coverage can be obtained.
6. Selective deposition can be obtained with proper design of the reactor.
7. The process is very economical because of its high throughput and low maintenance costs.

1.4 Limitations of CVD

Fundamental limitations of CVD are the chemical reaction feasibility and the reaction kinetics that govern the CVD processes. Technological limitations of CVD include the unwanted and possibly deleterious but necessary by-products of reaction that must be eliminated, and the ever present particle generation induced by homogeneous gas phase nucleation that must be minimized.

1.5 Dielectric Materials

A dielectric is a material of low dc electrical conductivity and hence a good insulator or storage medium of electric energy as in a capacitor. Dielectrics play an important role in the fabrication and development of semiconductor microcircuits. Their major functions have been for the isolating circuit elements, impurities, masking against oxygen and dopant diffusion, passivating and protecting device surfaces, insulating double-level conductor lines, and tapering or planarizing the device topography.

The requirements of these dielectric materials in the form of thin films for VLSI circuits for high density devices featuring linewidths in the low micron to submicron range, should have minimal structural defects and good step coverage. The particle density must be as low as possible, and the size of the particulate contaminants should not exceed 25% of the smallest feature size in the integrated circuit to avoid electrical failures of device reliability problems.

1.5.1 Requirements of Dielectric Materials for VLSI Technology

Dielectric films for insulating applications of multiple level VLSI devices must sustain relatively high dielectric breakdown fields, should have a low dielectric constant (to minimize the parasitic capacitance between conductors) and a high electrical resistivity, must have a low loss factor for high frequency applications, must be free of pinholes and microcracks and should have a low compressive stress and excellent adhesion properties. In addition, depending on the layer structure, some of the films must allow hydrogen to diffuse through to allow removal of interface states by annealing in hydrogen, and be able to block alkali ions. All films must be readily depositable at temperatures compatible with the device structural materials and device performance requirements, with excellent compositional control and good step coverage. There materials must be patternable by precision lithography and selective etching.

1.5.2 Desired Properties of Dielectric Materials

A. Electrical

- high dielectric breakdown voltage (1000 - 1500 V/μm)
- low dielectric constant to minimize parasitic capacitance (3.5 - 4.5)
- low dielectric loss factor
- high electrical resistivity (10^{16} - 10^{17} Ω-cm)

B. Chemical

- compositional controllability
- chemical stability
- gettering of alkali ions
- low hydrogen content. Not a source of outgassing
- depositable at low (compatible temperature)

C. Physical/Mechanical

- free of pinholes, microcracks, particulates, voids
- conformal step coverage with positive slopes
- low compressive stress
- uniform film thickness

- good adhesion to substrates
- barrier to alkali ions
- allowing hydrogen to diffuse
- patternable by precision lithography and selective etching
- fusible for thermal flow tapering or planarization.

1.5.3 Applications of Dielectric Materials in VLSI Technology

A. In device structures for

- isolation of circuit elements
- vertical insulation of high-temperature conductor levels in multilevel structures (polysilicon, silicides, refractory metals)
- vertical insulation of low-temperature conductor levels in multilevel structures (aluminum and its alloys)
- alkali ion and moisture barrier
- impurity gettering
- contour leveling or planarization
- over-metal top passivation

B. For temporary layers and processing aids as

- masking structures against oxidation
- gettering layers for impurities
- sacrificial material in lift-off patterning

1.6 BN as a Dielectric Material

Some of the attractive properties of BN are its low deposition temperature, high insulation, high passivation effects against moisture and the alkali metal ions, conformal step coverage, high crack resistance and chemical inertness. BN is not attacked by mineral acids. It starts dissociating at 2700°C in vacuum and is oxidized in air only at temperatures as high as 1200°C. It has a reported dielectric constant close to that of silicon dioxide and electrical resistivity in the order of 10^{14}ohm-cm with a dielectric strength in the order of 10^6 V/cm and an optical band gap of 4-6 eV. This makes a good material to study the electrical properties.

1.7 Borane Triethylamine Complex as a Precursor

Extensive work has been done on the chemical vapor deposition of BN thin films on various substrates including silicon, quartz, and glass. A wide range of precursors have been used to obtain these thin films which include diborane, borontrichloride, triethyl boron, dicarborane and borane triethylamine (TEAB) complex. TEAB has several advantages over many of the other precursors. Table 1.1 gives some of the properties of TEAB.

TEAB is a relatively non-toxic and non explosive substance and this obviates the need for expensive cabinets and a cross purging gas supply for safety reasons. However, TEAB has a low vapor pressure and hence has to be forced into the reactor under high pressure.

Table 1.1 Properties of TEAB

Chemical name	Borane triethylamine complex (TEAB)
Chemical formula	$(C_2H_5)_3N.BH_3$
Molecular weight (g/mol)	115.03
Specific gravity (g/cc)	0.777
Freezing Point	-3°C
Boiling point	97°C
Appearance	Colorless liquid
Vapor pressure	20 Torr at 97°C
CAS Registry number	1722-26-5

CHAPTER 2

REVIEW OF LITERATURE OF BN FILMS

2.1 Introduction

In this chapter a review of the deposition techniques of boron nitride thin films and their properties will be discussed. A brief review of the electrical characteristics, including the current-voltage, electrical resistivity and the dielectric constant of thin films in general and BN and SiBN films in particular will be discussed. Finally, the aim and scope of this work will be discussed.

2.2 Deposition Techniques

Thin films of boron nitride have been grown on various substrates including copper, steels, silicon, quartz, sapphire and fibers. The techniques used (Table 2.1) have included chemical vapor deposition (CVD) [1-9], low pressure chemical vapor deposition (LPCVD) [10,11], plasma assisted CVD [6,12-16], reactive sputtering [17,18], electron beam irradiation [19], ion beam deposition [20-22],ion plating and pulse plasma method [23-25]. Boron sources have included diborane [1-3,6,10,12], boron trichloride [4-8,14], borazine [11], triethyl amine borane complex [15,16] and dicaborane [9].

In this section a review of the synthesis of boron nitride by chemical vapor deposition and low pressure chemical vapor deposition techniques is done as it is relevant to the present work.

Table 2.1 Synthesizing techniques of boron nitride thin films

Technique	Reactants	Remarks	References
CVD	B_2H_6, NH_3, H_2, N_2	Deposition temp. 400-1250°C, max. Deposition rate at 800°C, clear, vitreous films	1 - 3
CVD	BCl_3, NH_3, H_2 (Ar)	Deposition temp. 250°-1250°C, films deposited below 450°C are unstable in moist atmosphere, transparent and smooth films are produced between 1000° and 1200°C	4 - 8
MFCVD	$B_{10}H_{14}$, NH_3	Stoichiometric films are deposited at temp. Of about 850°C	9
LPCVD	B_2H_6, NH_3	Physical and optical properties of the films formed at temp. 300°-400°C are stable and inert towards water and aqueous solutions	10, 12
LPCVD	Borazine	Films formed at temp. 300°-400°C react with atmospheric moisture	11
PECVD	B_2H_6, NH_3	Deposition temp. 1000°C, polycrystalline structure appears	6
PECVD	B_2H_6, NH_3	Deposition temp. 550°-620°C, amorphous structure	14
PECVD	$BH_3N(C_2H_5)_3$, NH_3	Deposition temp. 200°-350°C, amorphous structure, good electrical properties	15 - 16
Sputtering	B, BN, N_2 (Ar)	Films can be deposited without heating the substrate	17, 18
Electron beam evaporation	BN	Stable amorphous structure, deposition temp. 1050°C	19
Ion beam deposition	B, N_2, NH_3 (Ar)	Ion beam plating of e-beam evaporated boron	20
Ion beam deposition	$B_3N_3H_6$ (Ar)	Plasma decomposition	21, 22
Pulse plasma method	B_2H_6, B, N_2, H_2	Plasma decomposition, cubic structure	25

2.2.1 Synthesis by CVD and LPCVD Techniques

Many investigators [1-3] deposited BN thin films from diborane and NH_3 using an inert carrier gas according to the reaction

$$B_2H_6 + 2NH_3 = 2BN + 6H_2$$

Rand et al. [1] used many substrates such as Si, Ta, Mo, Ge and fused silica, at various temperatures ranging from 600°C to 1080°C. The typical deposition rates varied from 12.5 to 60 nm/min. in H_2 or He and 100 nm/min. in nitrogen. The dependence of the deposition rate on temperature and NH_3 to B_2H_6 ratio was found to be complex. The deposition rate exhibited a maximum at 800°C and it decreased as the NH_3/B_2H_6 ratio was increased from 10:1 to 20:1.

Murarka et al. [2] studied the growth process on silicon substrates. The deposition rate was proportional to the flow rate of B_2H_6 and to the negative fifth power of the flow rate of NH_3. For a fixed NH_3/B_2H_6 ratio, the deposition rate increased linearly with the flow rate. The deposition rate increased with temperature in the temperature range 400°C to 700°C, and at higher temperatures, the reaction was nearly independent of temperature.

Hirayama et al. [3] also used Si substrate, maintaining the substrate temperatures ranging from 700°-1250°C. The growth rate of the film was about 50nm/min. at 700°C.

Baronian [4], Motojima et al. [6] and Takahashi et al. [7,8] used BCl_3 and NH_3 with the following reaction

$$BCl_3 + NH_3 = BN + 3HCl$$

Baronian [4] deposited BN thin films on quartz substrates at temperatures ranging from 600°-900°C. Motojima et al. [6] used Cu substrates at temperatures in the range 250°-700°C. The films deposited at temperatures below 450°C were unstable in a moist atmosphere.

Takahashi et al. [7,8] studied in detail the effect of the substrate material on the growth process. According to their results, Fe and Ni were the favorite elements for forming BN crystalline deposits. The formation of the first layer of BN was initiated by a catalytic action of the Fe atoms.

Nakamura [9] proposed a new CVD method in the molecular flow region (MFCVD) for depositing BN films using $B_{10}H_{24}$ and NH_3 reaction gases at substrate temperatures between 300° and 1200°C. He has reported that the deposition of the films could be closely controlled by regulating the pressure of the source gases and stoichiometric BN films could be deposited at $NH_3/B_{10}H_{24}$ ratios of 20 or more at a substrate temperature.

Adams and Capio [11] and Adams [12] prepared BN films from B_2H_6 and NH_3 at low pressures and temperatures ranging from 250°-600°C. Adams [12] also prepared BN films by pyrolysis of borazine at a temperature ranging from 300°-450°C and reported that the films formed from B_2H_6 and NH_3 are inert towards water and aqueous solutions. In contrast the films formed from borazine react with atmospheric moisture.

2.3 Properties of Boron Nitride Films

In this section the mechanical, optical, chemical, thermal and electrical properties of BN films are discussed.

It is found that the structure of the BN thin films are amorphous or polycrystalline (hexagonal or cubic) depending on the method of synthesis. Table 2.2 gives a few details of the properties of BN films based on the method of synthesis. The density [12] of the BN films is 1.7-2.1 gm/cc.

Table 2.2 Properties of BN thin films

Deposition technique	Refractive index	Optical band gap (eV)	Dielectric constant	Electrical resistivity (Ω-cm)	Dielectric strength (V/cm)	Ref-erences
CVD	1.7 - 1.8	3.8	3.7	10^{14}	5×10^{6}	1
CVD	1.7 - 2.8	-	-	-	-	2
CVD	-	-	3.3 - 3.7	$10^{9} - 10^{10}$	10^{7}	3
CVD	1.9 - 2.0	5.83	-	-	-	4
CVD	-	5.8 - 6.2	-	-	-	5
CVD	-	-	-	-	-	6
CVD	1.65	-	-	10^{14}	-	8
MFCVD	-	5.9	-	-	-	9
PECVD	-	-	2.7 - 7.7	10^{9}	-	13
PECVD	-	-	3.5	-	7×10^{6}	15,16
Sputtering	-	4.9 - 5.6	3.8	-	-	17
Sputtering	1.6 - 1.9	3.3 - 5.6	-	-	-	18
Ion beam deposition	-	-	-	10^{10} - 10^{14}	-	22
Plasma pulse method	1.5 - 1.6	5.0	5.6 - 7.0	10^{16}	10^{6}	25

The chemical composition of the films depends on several experimental parameters. Films synthesized by r.f. sputtering[18] in argon gas discharge have an excess of boron and BN. However, by controlling the experimental parameters, stoichiometric BN thin films can be grown. It was also found that boron nitride thin films prepared by ion beam deposition method [20,21] contain a considerable amount of oxygen and those obtained from pulse plasma method [25] show the presence of microinclusions of B_2O_3 and boron. Some film react with moist atmosphere. the intrinsic cause of such a reaction was reported [1,16] to be due to the presence of oxygen at the time of deposition.

The IR spectrum of a film deposited on silicon shows two typical absorption bands. A strong asymmetrical band at 1400 cm^{-1} is attributed to B-N bond stretching. A weaker sharper band at 800 cm^{-1} is attributed to B-N-B bond bending. The broadness and frequency shifting of the BN stretching vibration band depend on experimental conditions. The adherence of the films depends on the substrate material and deposition conditions. However, the adherence of the films has been generally satisfactory. The films deposited at reduced pressure at 340°C have a lower stress at all NH_3 to B_2H_6 ratio is less than about 0.3; at higher ratios, the film stress is compressive. For the B-H-N structure [12], the hydrogen content affects the stress. When the hydrogen content is less than about 21 atom percent, the films are under tensile stress and, for hydrogen concentrations of about 24 atom percent, the films are under compressive stress.

The thermal stability of the BN films depends on the deposition conditions. For example, the films deposited by CVD [6] at above 600°C were stable, decreased in mass by 1-2 percent on heating and were stable in air at temperatures below 750°C. For films deposited at temperatures over about 1000°C, no changes were observed in the polycrystalline patterns even after a long treatment [3] in hydrogen or nitrogen for several tens of hours at 1250°C. However, amorphous films deposited below 1000°C were decomposed during heat treatment in nitrogen [3].

The boron nitride films are chemically stable and cannot be attacked by etching solutions except for phosphoric acid [1,3,12]. The etch rate of the film [3] is about 8 nm/min. in a solution of equal volumes [1] of deionized water and phosphoric acid at 130°C and 15 nm/min. in pure phosphoric acid at 180°C. The films can be etched easily in a CF_4-O_2 [12] plasma, but the etch rate depend on the deposition temperature of the film.

The optical band gap and the refractive index vary according to the experimental parameters and boron-to-nitrogen ratio. The reported values of the band gap lie in the range from 3.3 to 6.2 eV (Table 2.2) and the refractive index from 1.5 to 2.8. In the visible region, the stoichiometric BN film is highly transparent and colorless but, on increase in the boron-to-nitrogen ratio in the film structure, the color becomes pale yellow, deep brown or light golden [18].

BN films are good electrical insulators. Their electrical resistivity is about 10 Ω-cm at room temperature and 10^3 at 200°C. The dielectric constant is about 4. BN films have a low dielectric losses at frequencies ranging from dc to microwave. The dielectric breakdown field strength is about 10V/cm.

The chemical composition of the films prepared by LPCVD [10-12] differs from stoichiometric BN film and these films are called *borohydronitride* (B-H-N) films. Johnson et al. [26] reported that B_3NH films produced using LPCVD in a manner similar top that used by Adams and Capio [12] were susceptible to radiation damage from 1-3 KeV X-ray radiation. This would lead to pattern distortion and shorten the life span of the masks. They related the problem to hydrogen content of the film and there by the deposition temperature of the film. Levy et al. [27] showed that the heat treatment of the film resulted in the loss of the hydrogen bond to the ammonia at around 700°C and the loss of hydrogen bond to the boron at around 1100°C. The result indicated that the conduction follows the Frenkel-Poole emission mechanism. The current-voltage (I-V) characteristics of BN films are non linear. The conduction mechanism through BN films is either Schottky type (Poole-Frenkel) or space charge limited depending upon the conditions of the film deposition.

2.4 Applications

BN film can be used as an insulator in a metal-insulator-semiconductor (MIS) memory diode[3]. An n-type silicon substrate is chosen and thermally oxidized to form SiO_2 of 17 nm thickness over which a BN film of 50 nm thickness is deposited by LPCVD. Then Al is evaporated to get a structure of Al-BN-SiO_2-Si as shown in figure 2.1. This structure shows an anomalous shift of its capacitance-voltage (C-V) curve with applied voltage. applied to the Al electrode is more than +35V.

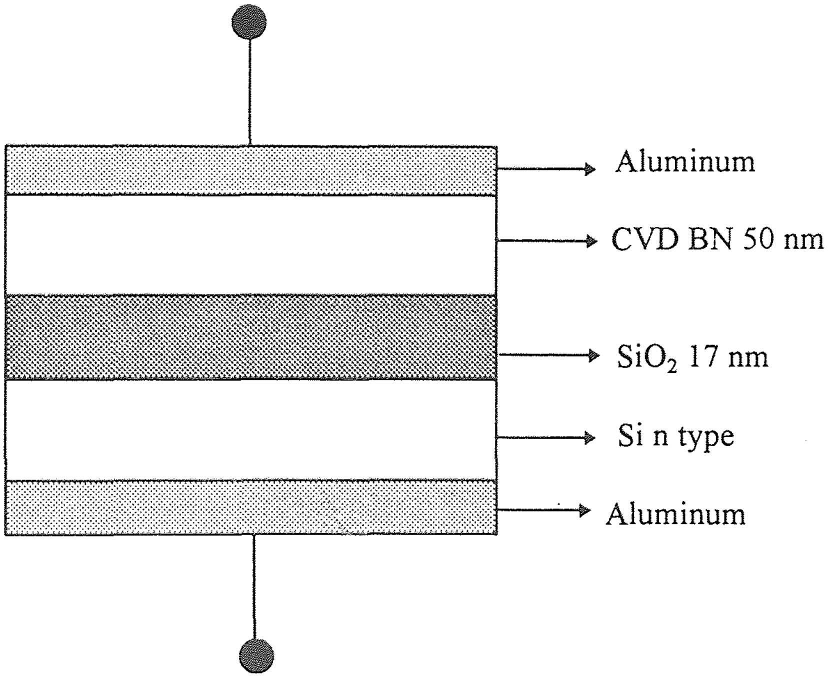

Figure 2.1 A typical MIS diode

When a negative voltage of more than 10V is applied to the Al electrode, the C-V curve begins to shift in the positive direction. The C-V curve saturates at an applied voltage of about -35V. Next if the positive voltage is applied to the Al electrode, the C-V curve begins to shift in the negative direction. The C-V curve saturates again when the voltage applied to the aluminum electrode is more than +35V.

BN films form a transparent substrate for X-ray lithography mask [12,28,29]. The BN mask is inexpensive and easy to fabricate, highly transparent to Pd L X-rays and dimensionally stable through all phases of mask processing. This mask is also optically transparent to facilitate reregistration.

BN films are useful as a restricted-area boron diffusion source. This method can be used to fabricate planar diodes using only one photomask. The n type Si wafers are thermally oxidized to about 300 nm, and the windows are opened in the silicon dioxide. Next a BN film is deposited. To diffuse the boron in the windows, the BN film must be decomposed. For this, the samples are heated in nitrogen atmosphere at 1100°C for about 120 minutes. Boron diffuses into the silicon through the windows, and the bare silicon surface appears on the windows. Then, to make ohmic contacts, Ni can be deposited directly by electroless plating on bare silicon surfaces of the windows and on the back face of the silicon wafer. Thus by these processes, planar diodes can be made by using only one photomask.

BN film coatings rate useful to increase the hardness of materials [20-22] as protective coatings against the oxidation of base materials.

BN thin films show a stable, strongly non-ohmic high field conductivity [1]. A film of about 100 nm thick (or thinner) may be used in integrated circuits as thin film varistors or voltage limiters.

BN films can be used as high quality insulating films [15,16] for MIS structures based on III-V compounds such as GaAs and these structures are suitable for high frequency device applications.

2.5 Dielectric Thin Films

As device operating speeds approach the gigahertz level, the signal transmission rate becomes limited by the capacitance between the interconnect layers as reflected in the delay constant [30]

$$RC = \rho_m \varepsilon_{die} L^2/d_{die}$$

where ρ_m is the sheet resistance of the interconnect, L is the interconnect length, ε_{die} is the dielectric constant of the interlevel dielectric (ILD), d_{die} is the thickness of the ILD, R is the resistance of the interconnect metal, and C is the capacitance of the ILD. It is evident from the relationship that a low RC constant can readily be achieved through material modification by reducing the resistance of the interconnect metal and the dielectric constant of the ILD.

A desirable ILD material should exhibit in addition to a low dielectric constant, low mechanical stress, high thermal stability and low moisture absorption. Several ILD candidates have been explored over the last few years. These have included fluorinated SiO_2 [31-35], fluorinated polyamides [36,37] and BN [38-41] films. Fluorine is the most electronegative and the least polarizable element. Therefore, incorporation of F reduces the number of polarizable geometry. These changes result in lowering polarizability of the fluorinated SiO_2 film itself, thus lowering the dielectric constant.

2.5.1 Fluorinated SiO_2 Films

Several reports [31-35] have indicated that the dielectric constant of silicon dioxide films can be reduced with increasing amounts of F in the films.

Usami et al.[31] used a parallel-plate electrode CVD system to deposit SiOF films using tetraethoxysilane (TEOS)-He-O_2-C_2F_6 gas plasma generated by r.f. power at 13.56 MHz at a temperature of 360°C and a pressure of 9 Torr. They found that the deposition rate and refractive index of the film decreases with increasing C_2F_6 flow rate. This suggested that the there is a change in the film composition and also a decrease in film density with increase in C_2F_6 addition. They suggested that the Si-O bond strength was influenced by Si-F bond formation due to the high electronegativity of fluorine was the cause of reduction of refractive index due to the structural changes in the film. The dielectric constant of the SiOF films were compared before and after annealing at 400°C in a hydrogen atmosphere for 30 minutes. Before annealing, the relative dielectric constant of the conventional PE-TEOS oxide was 4.9. this value was higher than that of thermally grown silicon dioxide (3.9). This result is due to the presence of highly polarized compounds such as Si-OH and H_2O in the film. With increasing fluorine concentration, however, the relative dielectric constant decreased. It is supposed that polarization of Si-O bonds was changed with the presence of Si-F bonds due to the high electronegativity of fluorine. After annealing the relative dielectric constant was lower (4.5) than that before annealing at all fluorine concentration indicating that the highly polarized compounds such as Si-OH and H_2O content in the films decreased even though a small amount of fluorine desorbed from the film. The least dielectric constant of 3.6 was obtained at 14 atomic % fluorine.

2.5.2 Fluorinated Polyimides

Fluorinated polyimides [36,37] have also been investigated as potential ILD materials because of their attractive thermal, mechanical and electrical properties. Thin polymer films have been found to align with their chain axes preferentially in the plane of the film. This results in an anisotropy in the refractive index and dielectric constant in the plane of the film as compared to out of the plane. While anisotropy in the dielectric constant is difficult to measure experimentally, anisotropy in the refractive index is relatively simple to measure using polarized incident radiation. The primary means of reducing the dielectric constant and refractive index has been fluorination of the polymer backbone. This has been achieved by incorporation of hexafluoro groups and by aromatic substitution of fluorine atoms, trifluoromethyl groups, fluorinated alkoxy side chains, and more recently, pentafluoro sulfur groups. Reduction of dielectric constant in polyimides has also been achieved by introducing fluorine-containing additives and by blending Teflon into the bulk polyimide material. Control of the refractive index of polyimide waveguide materials has been achieved through copolymerization of fluorine containing monomers. It is believed that the dielectric constant and refractive index of fluorinated polyimides are reduced by a combination of mechanisms. First, the electronic polarizability is reduced through the addition of fluorine-carbon bonds. In addition, interchain charge transfer complexation and associated chain packing are impeded by bulky fluorinated side groups, by kinks in the polymer backbone, and by spacer groups. Low refractive indices in fluorinated polyimides can be accurately predicted by current property prediction techniques. This suggests that it is the fluorine atoms and the bonds in the polymer repeat unit that have the largest effect in reducing refractive index. As a result of the preferential alignment of the most polarizable groups in the polyimide, i.e., the main chain phenyl rings, control of refractive index in polyimides in and out of the plane of the film by introducing orientation into the polymer film, increases the refractive index in the direction of orientation and reduces normal to the direction of orientation.

D.C.Rich et al. [36] polymerized thick free standing polyimide films in dimethyl-acetamide and solvent cast on glass and studied the refractive indices and optical anisotropies of these low dielectric polyimides. They concluded that refractive index decreases in polyimides with increasing fluorine content. This was primarily the result of a decrease in electronic polarizability associated with the added carbon-fluorine bonds. They also reported that the refractive index in low dielectric constant polyimides could be reduced and controlled in and out of the plane of the film by inducing preferential alignment of the polymer chains. There was little preferential in-plane alignment of the polymer chains in the films either, due to high thickness of the films or lack of a tendency of these materials to order in the plane of the film. Dielectric constant values in the range of 2.7 to 3.6 have been reported.

In another work by Y.S. Negi et al. [37] on both fluorine and non-fluorine based polyimides, showed that low dielectric constants were observed for fluoro polyimides, while non-fluoro polyamides had higher dielectric constants.

2.5.3 BN and SiBN Thin Films

Recent publications [38-41] have reported on the use of plasma enhanced chemical vapor deposition (PECVD) to synthesize BN and SiBN as potential low ε materials.

Maeda et al. [38] deposited amorphous SiBN ternary films using a parallel plate electrode reactor using a SiH_4-B_2H_6-NH_3-Ar gas mixture at a frequency of 13.56 MHz to obtain low dielectric constant films. Strong and broad absorption bands were seen at wavenumbers 890 cm^{-1} and 1320 cm^{-1} in the IR absorption spectrum corresponding to Si-N and B-N lattice vibrations respectively. The refractive index was found to decrease with increasing B atomic ratios. An observed value of 1.71 obtained from stoichiometric boron nitride was similar to hexagonal like amorphous boron nitride films. The static dielectric constant (at 1MHz) monotonically decreased from $6.8\varepsilon_o$ of silicon nitride to $3.0\varepsilon_o$ for stoichiometric boron nitride with increasing boron atomic ratio. The optical dielectric constant also decreased with increasing boron atomic ratio to obtain a value of $2.9\varepsilon_o$ for BN. Thus the difference between the static and the optical dielectric constants was extremely small for BN films while the static dielectric constant was 1.75 times larger than the optical one for Si_3N_4. The I-V characteristics of SiBN films indicated that for silicon nitride the carrier transfer follows the hopping conduction and bulk limited Poole-Frenkel conduction in the lower and higher electrical field regions respectively. The films thus had low dielectric constant, good insulating characteristics, conformal step coverage and wet proof characteristics. The IR spectrum exhibited that 4-coordinate Si atoms are substituted by 3-coordinated B atoms with increase in B atomic ratio. Also a large number of bonded hydrogen atoms are incorporated in the films. Subsequent work done by the same authors [39,40], the SiBN films were doped with oxygen. They found out that in the [O]/2[Si] < 1 region, the dielectric constant decreases and the breakdown strength increases with increasing oxygen atomic ratio because doped oxygen atoms preferentially combine with Si atoms and stable and highly insulating Si-O bonds are formed. Conversely, in the [O]/2[Si] > 1 region, the dielectric constant increases and the breakdown strength decreases with increasing oxygen atomic ratio because excess oxygen atoms combine with B atoms, and instable and hygroscopic B-O bonds are formed. The lowest dielectric constant is obtained in oxygen doped SiBN films of which [O]/2[Si] nearly equals unity under certain [Si]. In addition, a lower dielectric constant is obtained under lower [Si].

CHAPTER 3

EXPERIMENTAL PROCEDURE

3.1 Introduction

Boron nitride thin films with varying composition were synthesized in a LPCVD reactor with a liquid injection system adjusting various parameters including temperature, pressure, gas composition and time of deposition. Fourier transform infrared (FTIR) analyses were done on the synthesized films to examine the vibrational modes of the deposited films. Stress on the films was measured and calculated by a the principle of radius of curvature difference. Refractive index and thickness of the films were measured by ellipsometry and interferometry respectively. The optical transmission of the films were measured using a UV-visible spectrophotometer. The current-voltage, capacitance-voltage, resistivity and the dielectric constant of the films were measured.

3.2 LPCVD Reactor

The deposition reactor is schematically shown in Figure 3.1. This reactor was manufactured by Advanced Semiconductor Materials America Inc.(ASM America, Inc.) as a poly silicon micro-pressure CVD system. The horizontal reaction chamber consists of a 13.5 cm diameter fused quartz tube and a 144 cm long encapsulated with a three-zone, 10 kwatt, Thermco MB-80 heating furnace. The process tube door was constructed of a 300 series stainless steel, with a side hinge and sealed with an O-ring. At one end the liquid precursor can be injected from a stainless steel bubbler into the reaction chamber through a precalibrated capillary tube and an air operated pneumatic valve. The flow of ammonia into the reaction chamber is controlled by a MKS mass flow controller. A spare nitrogen mass flow controller was installed to incorporate any necessary additional reactant gas into the chamber or for backfilling. This spare controller could be calibrated for the gases other than nitrogen.

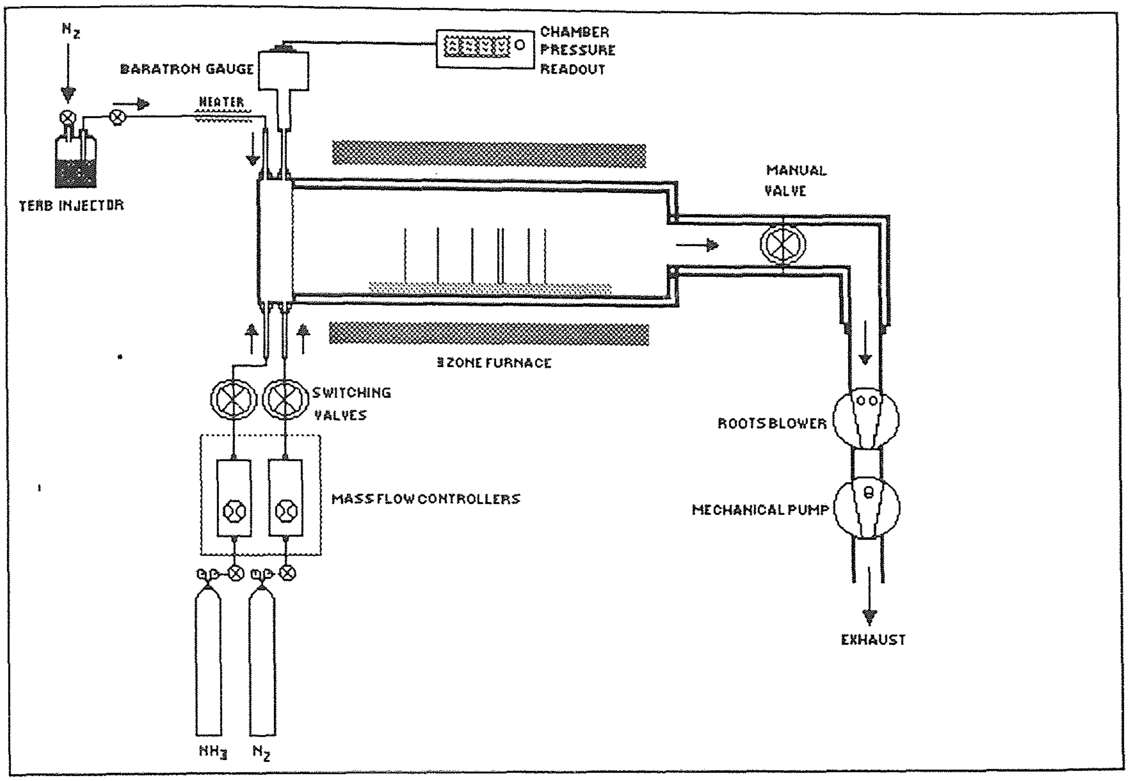

Figure 3.1 Schematic representation of the LPCVD reactor

The other end of the reaction chamber is connected to a vacuum station comprised of a Leybold-Heraeus Trivac dual stage rotary vane pump backed by a Leybold-Heraeus roots pump to create the necessary vacuum in the system. An oil filter system is used to filter unnecessary particles from oil and thereby increasing the lifetime of the pump. End caps designed for this reactor have a provision for cold water circulation to avoid overheating of the O-rings. A ceramic tube was setup between the chamber and the heater to enhance the radiation heat transfer thus reducing the temperature deviation through the reaction tube. The temperature was kept constant across all zones and confirmed using a calibrated K type thermocouple. Mass flow controller set points were programmed with a MICON 3 microprocessing controller which produces the set point voltage and automatically monitors the flow vs. the programmed flow limits. The pressure in the reactor is monitored with an automatic exhaust valve and measured at the reactor inlet using a capacitance manometer (13 Torr MKS baratron pressure gauge).

3.2.1 Liquid Injection Mechanism

The liquid injection system, designed and fabricated in-house [42,43], consists of a stainless steel bubbler connected to a precalibrated capillary tube fastened onto the reaction chamber. The flow rate is inversely proportional to the length of the capillary, while proportional to the pressure differential and the cross sectional area. The injection system has filters for both nitrogen purge (140 μm) and liquid precursor (7 μm) to reduce capillary blockage. The bubbler is always maintained at a positive pressure to restrict oxygen leak into it.

The TEAB complex liquid precursor used as a source of boron can slowly react with oxygen and forms an undesirable white powder contamination and hence requires handling in an inert glove box. Except otherwise noted, the flow rate of the TEAB precursor was maintained at 17 sccm using a pressure of 6 psi gauge throughout the experiments.

3.3 Experimental Setup

3.3.1 Leakage Check

A leak would result in a change in the deposit structure (due to oxygen) and could result in haze depending on the size of the leak, therefore a leakage check in the CVD is an important step before making an experiment [44]. When carrying out leak check, all pneumatic controllers and gas regulators should be fully open to the gas cylinder main valves. The capillary is disconnected and the inlet is sealed with a plug because it is not possible to create vacuum in the capillary in the limited time period. After pumping the reaction system for a whole day, closing the outlet valve of the chamber, the pressure increasing rate was measured at a fixed period of time in the chamber to obtain the leakage rate. For this LPCVD system, the leakage rate deviated from 0.13 to 2 mTorr/min. Depending on the chamber condition a very low leak rate for a new chamber and higher leak rate for a chamber after long time in service. However, the leakage rate in the system was basically good.

3.3.2 Calibration of Gas Flow System

The flow rates for the reactant gas NH_3 and the inert gas N_2 were calibrated by noting the increase in pressure in the reaction chamber with increase in time (the vacuum outlet being sealed). Using the ideal gas law, PV = nRT, the following formula could be deduced to calibrate the flow rate.

$$\frac{dV}{dt} = \left(\frac{Vr}{760}\right)\left(\frac{273}{Tm}\right)\left(\frac{dP}{dt}\right)$$

dV/dt is the is the flow rate of the tested gas in sccm, V_r is the pre-calculated volume of the reactor (20,900 ± 600 cm^3), T_m is the measured chamber temperature in kelvin and dP/dt is the rate of pressure increase. The tested gas in the vacuum conditions considered as an ideal gas and the reaction chamber was evacuated for several hours before testing. After setting up the flow rate, the gas regulator was opened to introduce the gas flow into the chamber, then the outlet valve of the chamber was closed and the pressure difference in the chamber was measured to obtain the rate of pressure increase. The real flow rate of the tested gas thus can be calculated using the above relation. The accuracy of this calibration involves the gas flow rate, the time interval, and the condition of the chamber should be carefully controlled. A smaller gas flow rate causes a slower pressure increase and thus leads to an easier detection of pressure increase and hence more accurate calibration. A longer time interval for calibration and a good vacuum condition in the chamber are also favored in the accuracy of calibration.

3.3.3 Calibration of Liquid Injection System

Since the vapor pressure of the TEAB complex is very low (12 Torr at 97°C), it is difficult to obtain a flow rate by the previous method. Therefore, another calibration procedure is described to calibrate the flow rate. The liquid is collected from the capillary and the weight of this at a fixed pressure drop is measured and the weight consumed per minute at this pressure drop was determined. The ideal gas law was used to calculate the vapor volume which could be produced at STP in order to obtain the value in sccm. A calibration of the capillary is necessary before each experiment to ensure that the capillary is devoid of any contaminants.

3.4 Deposition Procedure

Boron nitride films were deposited on (100) oriented single crystal, single-side polished Si wafers (obtained from Silicon Sense Inc.), and fused quartz wafers (obtained from Hoya, Japan). The details of the Si wafers is given in Table 3.1.

The wafers are labeled and accurately weighed (up to 4 decimal places) using an electronic balance. These wafers are then placed on a quartz boat. The wafers used to measure the stress on the film are placed back-to-back at a distance of 12.5 cm from one end of quartz boat and the quartz wafer at a distance of 4 cm from the stress monitors in all the experiments. The boat was placed in the reaction chamber at a distance of 54 cm from the loading end.

Table 3.1 Specifications of the Si wafer

Source	Silicon Sense Inc.
Diameter	100 mm
Orientation	<100>
Thickness	525 ± 25 μm
Type/Dopant	p/Boron
	n/Phosphorus
Resistivity	5 - 15 Ω-cm
Grade	Test

A low pressure is maintained inside the chamber using the vacuum pumps. TEAB is injected into the reaction chamber through the precalibrated capillary tube. Time of deposition was varied according to the required film thickness. Among the deposition parameters recorded were the background pressure, reaction temperature, flow rates of the reactants and the deposition time. Experiments were performed to change the stoichiometry of deposited films by adding ammonia to the amine complex in the reactor. The deposition time was changed in each case so that the thickness of the film was approximately maintained at about 1500Å.

Samples are allowed to cool to room temperature and the wafers are removed from the reactor by introducing nitrogen to fill the vacuum chamber and rise the pressure to atmospheric pressure. The samples are then weighed and the deposition rate can be calculated by knowing the mass gain (mg/hr) due to deposition. Samples were observed in an optical microscope for the presence of microcracks and for gas phase nucleation.

Fourier transform infrared (FTIR) spectra of the films obtained from Perkin - Elmer 580 were observed for B-N, B-N-B vibration modes and the presence of N-H, C-H bonding. Stress analysis was conducted to determine the stress developed in the film on the silicon substrate based on an indigenously fabricated laser beam equipment. The principle being the change in the radius of curvature of the film before and after deposition. Stress is calculated using Stony's formula

$$\sigma_s = ED^2/6(1-\nu)Rt$$

where E and ν are Young's modulus and Poisson ratio of the substrate. D, t are the substrate and film thickness' respectively, R is the radius of curvature of the composite.

By convention R is negative for a complex wafer surface (compressive film stress) and positive for a concave wafer surface (tensile film stress). In the present set of experiments for the wafers used and considering the geometry of the instrument used, the equation reduces to

$$\sigma_s(\text{MPa}) = 12.3R'/t\ (\mu\text{m})$$

where R' is the difference of the deflection of the projected laser spots after and before deposition.

Refractive index of the boron nitride films was determined using Rudolph Research/Autodec ellipsometry. The measurement technique is mainly concerned with the measurement of changes and the state of polarization of light upon reflection with the surface It employs monochromatic, plane polarized light with its plane of polarization 45° to the plane of incidence. When the elliptically polarized light is reflected from an absorbing substrate its state of polarization is changed. The ellipticity of the reflected beam is determined by the relative phase difference δ and azimuth ψ. An in-built computer program numerically solves the equations generated by these δ and ψ and the refractive index and the thickness of the film is obtained. In all the experiments the angle of incidence was maintained at 70° and the wavelength at 5461Å. Readings were taken at 5 places on the wafer and was averaged out.

The thickness of the films were measured using Nanometrics Nanospec/AFT nanospectrometer. The average refractive index obtained from the ellipsometer for that particular wafer was fed in and the thickness was measured in 5 places and averaged out.

X-ray diffraction patterns were studied to find the structure of the deposited films using IBM PC based Rigaku diffractometer. The optical transmission of the films were measured using a Varian DMS 300 UV/visible spectrophotometer over a range of wavelength from 190nm to 900nm. This also gives an approximate estimation of the optical band gap of the semiconducting BN thin film.

3.5 Electrical Characterization of BN Thin Films

3.5.1 Metallization

To study electrical characteristics of the synthesized films, the films were coated with pure Al. This was done in an evaporator, and the important parameters of deposition is given in Table 3.2. A mask is used to obtain Al dots of diameter 300μm and 600μm on the boron nitride film, while a uniform coating of Al is deposited on the back surface (Si surface of the stress monitor).

Table 3.2 Parameters for metallization of BN thin films

Base pressure	10^{-6} Torr
Heating source	Tungsten filament (resistance heating)
Evaporating source	Al wire
Purity of evaporating source	99.9999% (Al)
Rate of deposition	50 Å/min.
Ultimate thickness of deposit	900 Å
Substrate temperature	room temperature
Distance between the filament and the substrate	200 mm
Size of the dots	300 μm and 600μm diameter

3.5.2 Capacitance - Voltage Measurements

Capacitance - voltage (C-V) measurement was done for the films on both the p-type and n-type Si substrates. All samples went through a forming gas annealing at 450°C for 30 minutes after evaporation of Al dots through a shadow mask. The back side BN was removed by plasma etching (if necessary) and Al was deposited for back contact as explained in the previous section. The dielectric constant of the BN films were measured at five places and the breakdown voltage was determined. Subsequently, a bias stress study was made by applying a ±1MV/cm for 2-5 minutes at room temperature and C-V measurements were done after each polarity of stress. Bias-temperature stress measurements were also made to find out if there are trapped charges in the insulator. This was done by applying a positive and negative polarity of 0.5MV/cm for 10 minutes at 120°C. To find out the nature of the charges bias-temperature aging studies were done on the samples. The flat-band voltages were determined under various bias-temperature stresses. The above study was done on both p-type and n-type wafers. Finally a bias temperature stress cycle study was done by applying a positive 1MV/cm at 120°C and the polarity was reversed to a negative 1MV/cm at the same temperature and the C-V characteristics were determined.

3.6 Overview of Basis of the Present Work

Before going into the findings of the present work, for the sake of completeness and better understanding, a brief review of the research done [42,43] on the synthesis and characterization of boron nitride thin films over a series of temperature from 300° to 850°C using TEAB and ammonia as the precursors is discussed. Based on these results, further work was done by varying the flow ratio of ammonia and TEAB to study the growth kinetics of the reaction. In figure 2.2, the variation of growth rate of BN as a function of temperature is shown.

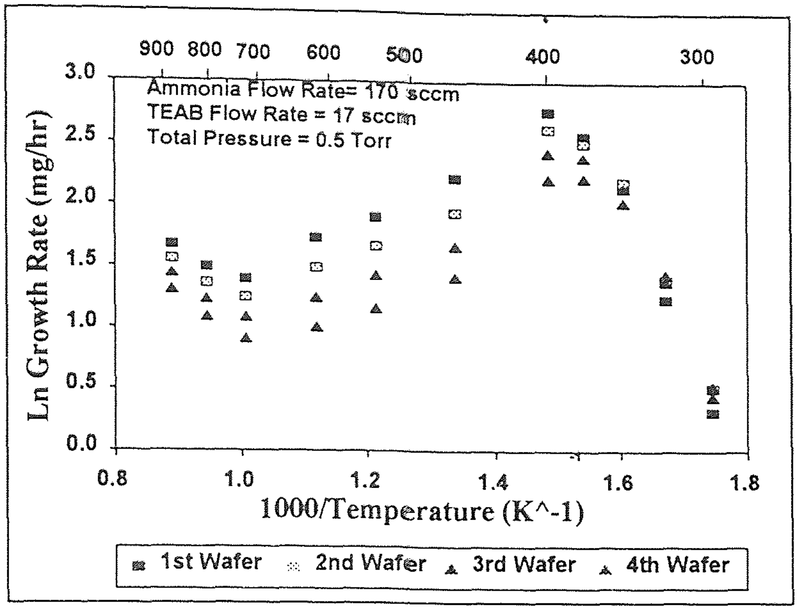

Figure 3.2 Temperature-growth rate relationship for depositing BN thin films on Si wafers

3.6.1 Kinetics of Film Growth

At a fixed total flow rate of 187 sccm, NH_3/TEAB ratio of 10/1 and total pressure of 0.5 torr, the kinetics of film growth were investigated in the temperature range of 300° to 850°C. The deposition rate plotted over the range of 300° to 350°C exhibits an Arrhenius behavior of 22 kcal/mol. The addition of NH_3 lowered the minimum deposition temperature by around 300°C. Between 350° and 400°C, the curve changes slope reflecting the onset of the changes in reaction mechanism. It is observed that at these low temperature region, the reactants did not become sufficiently hot prior to their flow over the substrates: as they travel toward the exhaust they become warmer leading to increased deposition rates on the last wafer along the flow. In the range between 400°C and 700°C, the deposition rate decreases monotonically due to the increased contribution of depletion effect. Above 720°C, a slight increase in deposition rate is assumed due to the changes in the gas phase chemistry which are also reflected in the changes in the film composition, density, stress, color etc. The shape of the curve is complex and consistent to the curve of the refractive indices reflecting the chemical mechanism of the processes and the composition of the films are strongly dependent on the temperature.

In the present study 3 temperatures were taken from the above graph at 400°C, 475°C and 550°C and the TEAB ratio was maintained at 17sccm using a liquid injection setup as explained earlier. The flow rate of NH_3 was varied to obtain ratios of 10:1, 20:1 and 30:1 for these temperatures. To obtain higher ratios of 40:1 and 50:1 of NH_3:TEAB, the TEAB flow rate was reduced to 12 sccm so that the above ratios could be achieved [45].

The effect of flow ratio and temperature with the thickness, density, stress, refractive index, optical absorption coefficient, dielectric constant, I-V, and C-V characteristics were studied.

CHAPTER 4

RESULTS AND DISCUSSION

4.1 Introduction

The results of boron nitride thin films synthesized on Si and quartz substrates at a constant pressure of 0.5 Torr, at 3 temperatures 400°C, 475°C and 550°C at various ammonia to TEAB flow ratios are described in this Chapter. The deposition time was varied to obtain an average thickness of about 1500Å to facilitate electrical measurements.

The films appeared light brown to golden yellow on quartz wafers and were reasonably transparent. A more detailed description of the optical transparency and the absorption coefficient of the film is described later in this Chapter. There were no cracks on the film surface and consistently, in all films the thickness varied by about 200Å at the bottom - near the primary flat of the Si wafer and at the top (the top being thicker). However the films were uniform over majority of the substrate. When observed under the optical microscope, no traces of gas phase nucleation could be observed.

In the subsequent sections the characterization of films in terms of IR, UV and visible absorption spectroscopy was done to understand the nature of the bonding and contamination of films, if any, identified by impurity peaks in the spectra. Auger analysis was also done to find out the exact composition of the film. The effect of flow ratio and temperature with the thickness, density, stress, refractive index and optical absorption coefficient are discussed. Finally, the electrical characterization of the films is discussed.

4.2 FTIR Spectroscopy and Auger Analysis of BN Thin Films

The typical FTIR absorption spectra of boron nitride thin films (Figure 4.1(a)) at 400°C, 0.5 Torr pressure and a flow ratio of NH3/TEAB = 10/1 showed absorption peaks at wavenumber of about 1350 cm^{-1} corresponding to the B-N vibration mode, and a small peak close to 800 cm^{-1} corresponding to the B-N-B vibration. Apart from these major peaks, B-H peak at wavenumbers 2500 cm^{-1}, and N-H peaks at wavenumbers 3200 cm^{-1} and 3400 cm^{-1} C-H peak at 2900 cm^{-1} could be seen. Also a contamination O-H peak can be seen at about 3600 cm^{-1}.

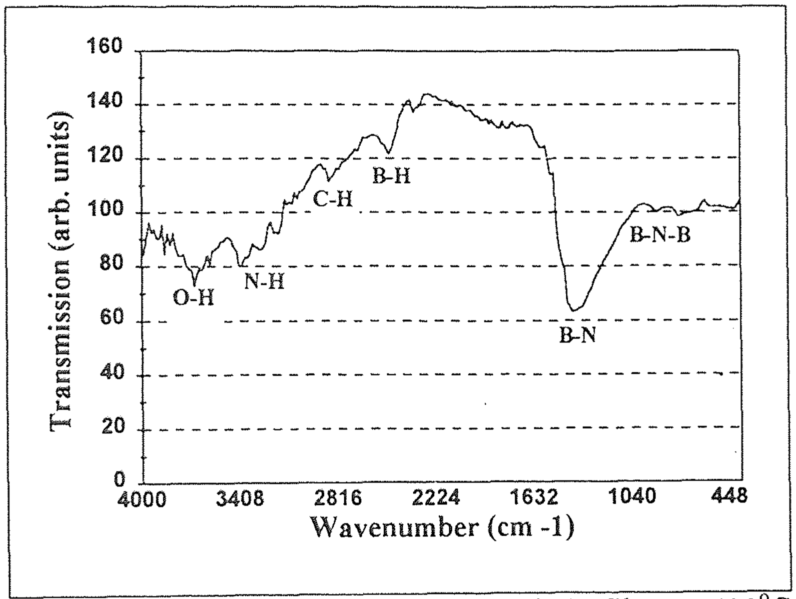

Figure 4.1(a) Typical FTIR spectrum of BN films at 400°C

It can be seen that the B-N and B-N-B absorption peaks increase with increasing flow rate of ammonia at all the temperatures under consideration. In addition, with increase in temperature, at 550°C (Figure 4.1(b)), the peaks at wavenumbers 3400 cm^{-1}, 3200 cm^{-1}, and 2900 cm^{-1} and 2500 cm^{-1} corresponding to N-H, C-H and B-H vibration modes respectively disappear.

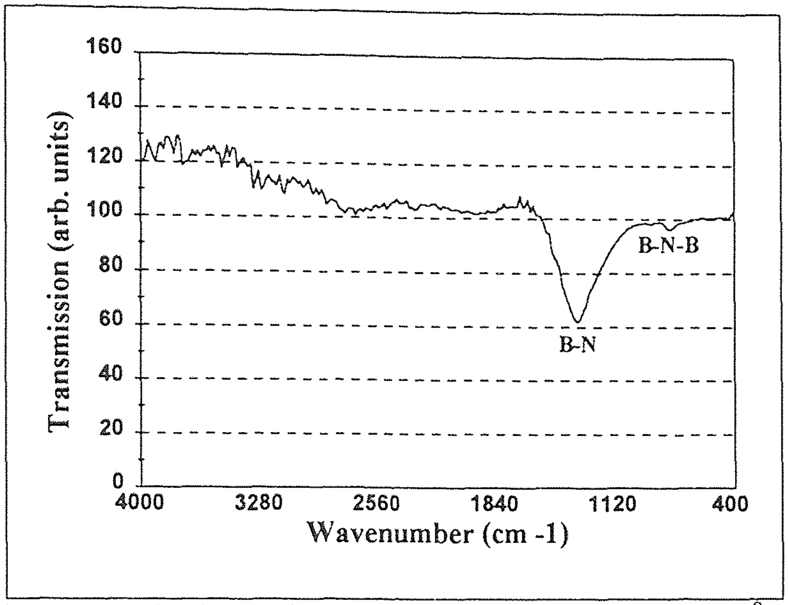

Figure 4.1(b) Typical FTIR spectrum of BN films at 550°C

Figure 4.2 shows the shift in the peak position with increasing temperature at a constant flow ratio of NH_3/TEAB = 30/1. This indicates that the stoichiometry of the film is changing with increasing flow ratio. As the thickness increases, the intensity of the peak also increases. Auger analysis indicated a carbon percentage of about 8, but from the infrared absorption spectra, no C-C or C-H peaks at high temperatures and at high flow rate could be identified. The asymmetric shape of the carbon peak in the Auger analysis reveals that it is not bonded in any carbide form, rather in an elemental form.

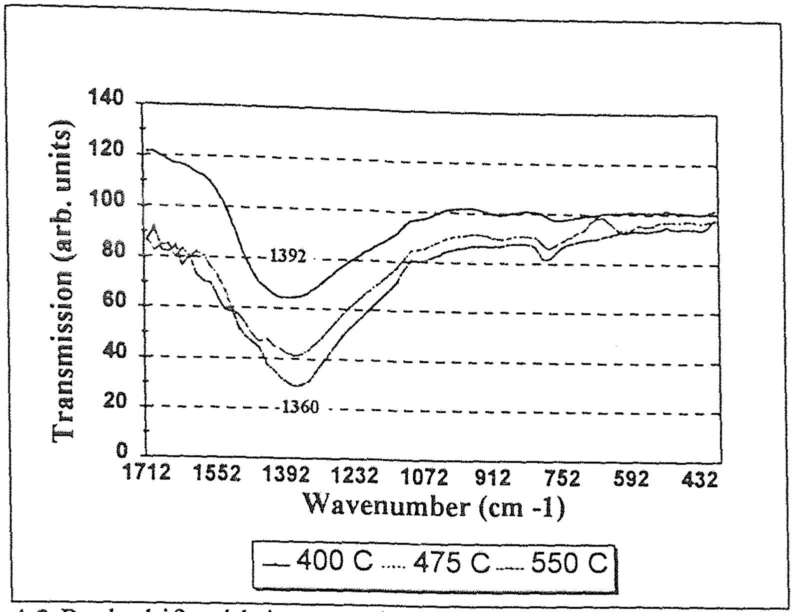

Figure 4.2 Peak shift with increase in temperature at NH_3/TEAB ratio 30/1

Thus, FTIR is insensitive to the presence of carbon in the film. Thus the film is essentially amorphous carbon containing boron nitride. Figure 4.3 shows the Auger depth profile of the chemical constituents of BN thin films.

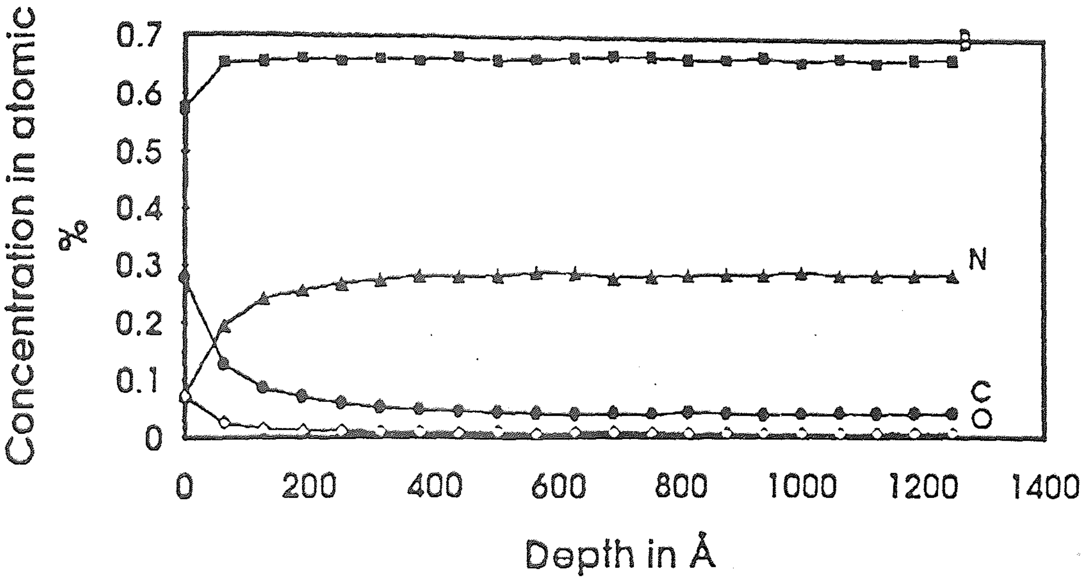

Figure 4.3 Auger depth profile of the contents of BN films

4.3 UV/Visible Spectroscopy of BN Thin Films

The optical transmission of the boron nitride film deposited on quartz wafers were studied using a UV/Visible spectrophotometer. Typical optical transmission curve is shown in Figure 4.4.

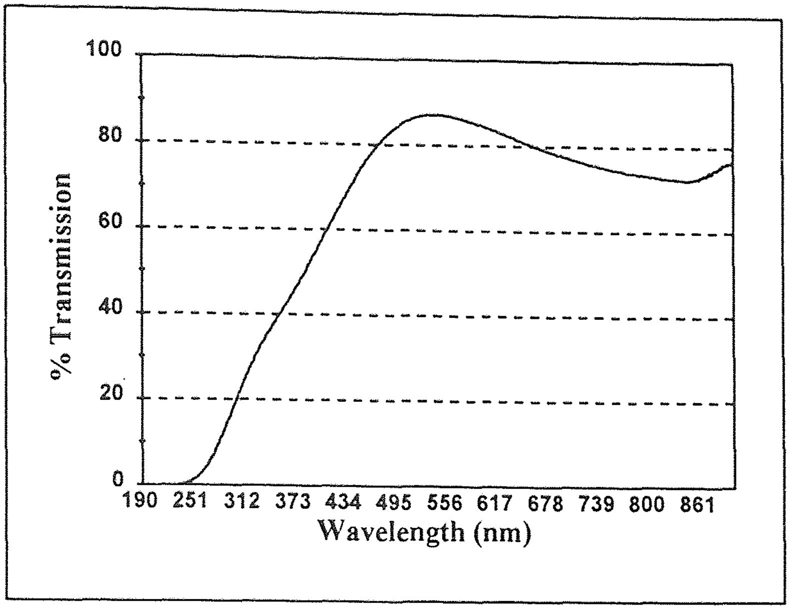

Figure 4.4 Optical transmission of BN thin films

The optical transmission of the films synthesized varied from 92% to 72% at 633nm (corresponding to red light) depending on the thickness of the film and the stoichiometry of boron, nitrogen and carbon ratios in the films. As the wavelength is reduced from the visible region to the ultra violet region (approx. < 300nm) the transmission goes down and at about 210nm the light is completely absorbed. This is typical of a semiconducting material with the electrons jumping from the valence band to the conduction band as a result of the excitation of the electrons due to this supplied quanta of energy (by a photon). Hence the optical band gap of this semiconducting material could be estimated.

X-ray diffraction study was done on these Si wafers and it showed no peak corresponding to hexagonal or cubic phase of BN. It just showed a big Si peak due to the substrate. Thus the BN films are essentially amorphous with no long range crystallographic order.

4.4 Effect of Flow Ratio of NH_3/TEAB

4.4.1 On Film Thickness

In all cases the film thickness was maintained at about 1500 Å to facilitate the electric characterization viz., the I-V characteristics as well as dielectric constant measurements. To this effect, the time of deposition was varied. However, all the values of thickness has been normalized to one hour of deposition time for comparative purposes.

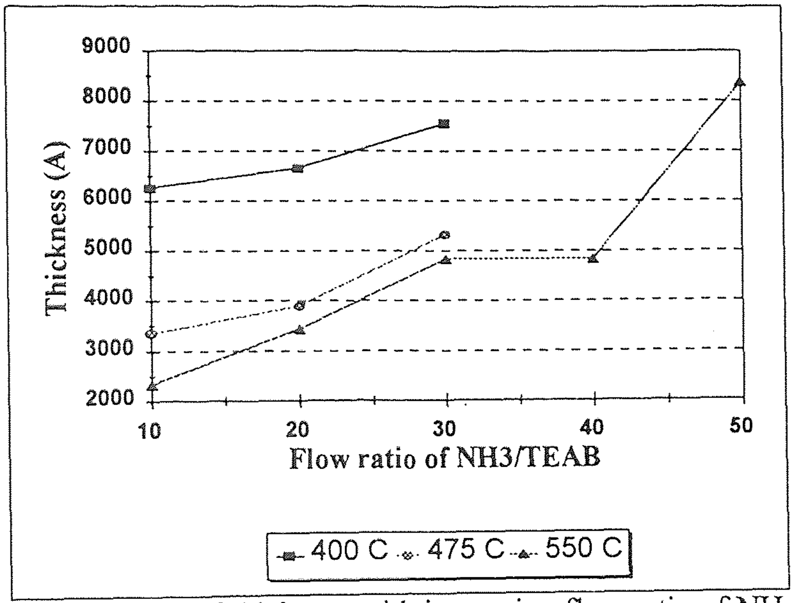

Figure 4.5 Variation of thickness with increasing flow ratio of NH_3/TEAB

Figure 4.5 shows the variation of thickness with increase in ammonia flow rate. The thickness of the film increases with increasing ammonia flow rate. This is primarily due to change in stoichiometry in the film. This can be confirmed by the peak shifts in the IR spectrum as well as Auger analysis.

In all the cases, there was higher deposition rate in the stress monitor facing the loading end - also the entry of the precursors - and lower deposition rate in the wafer facing away from the loading end in the stress monitors. At lower flow rates of NH_3/TEAB, the thickness' of the stress monitors are comparable but, with increasing ammonia flow, the depletion effect is much more predominant (Figure 4.6).

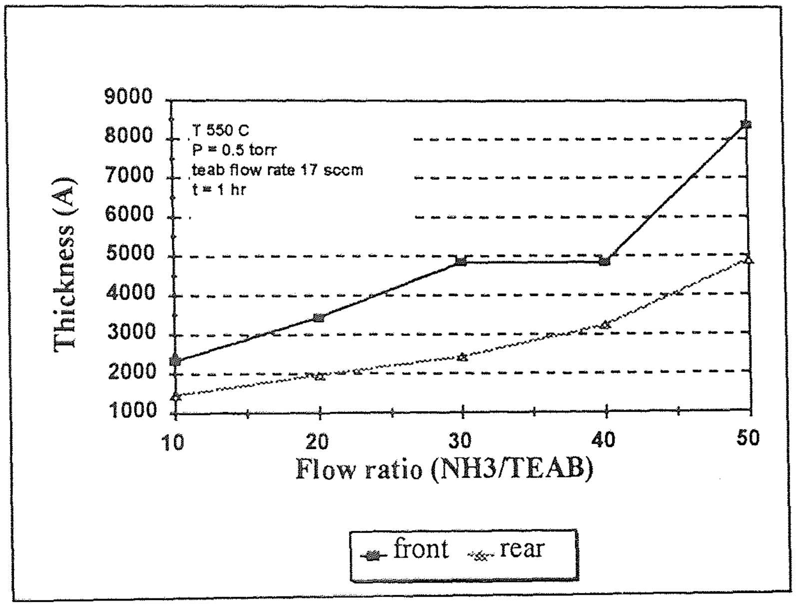

Figure 4.6 Effect of depletion on back-to-back stress monitors at 550°C

4.4.2 On Film Density

The film density is calculated as the ratio of the weight gained by the film to the thickness of the film for that particular wafer. The thickness' used were based on the values obtained by the Nanospectrophotometer. It is seen that the density decreases with increase in flow ratio of ammonia/TEAB (Figure 4.7).

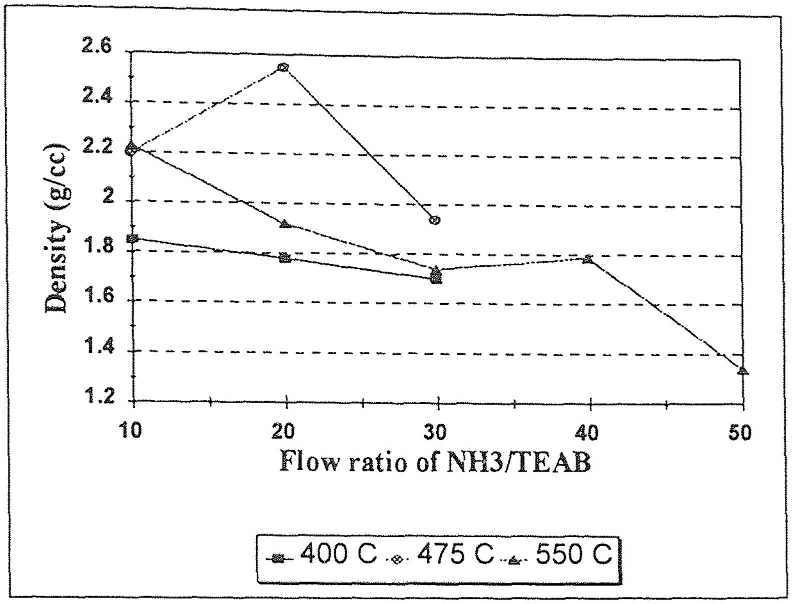

Figure 4.7 Variation of film density with increasing flow ratio of NH_3/TEAB

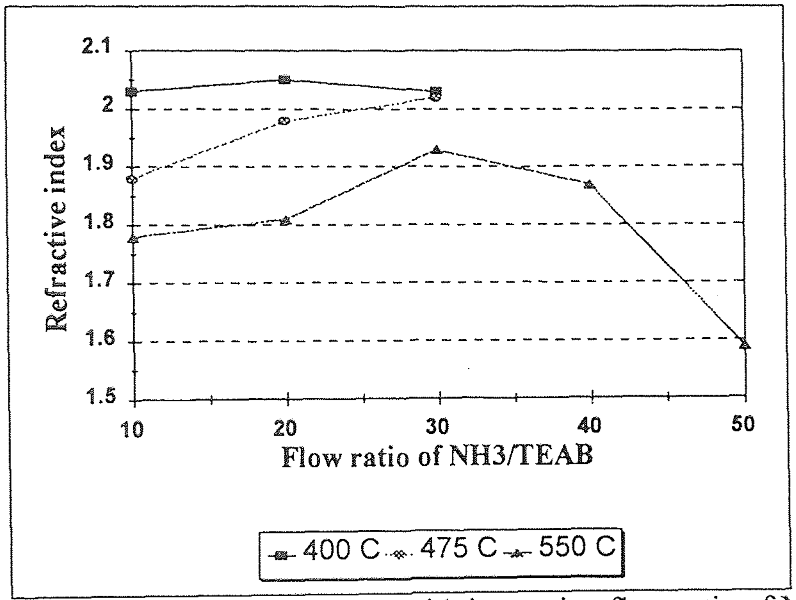

Figure 4.8 Variation of refractive index with increasing flow ratio of NH_3/TEAB

This could be a result of more porous films. However, gas phase nucleation could not be seen in the optical microscope. As seen from the Auger study, the presence of carbon makes the refractive index measurements and hence the thickness measurements difficult. Hence the reason for low density could not be explained with certainty. However, in most LPCVD processes, there is a variation of the density of the film is common due to the non-stoichiometric films.

4.4.3 On Refractive Index

Figure 4.8 shows the variation of the refractive indices of the film with the flow ratio. With increase in the ammonia flow rate, the refractive index increases. The increase is marginal though and the indices hover around 1.8 to 2.0. Interestingly, when the flow ratio was increased drastically at 550°C to 40:1 and 50:1, the refractive index dropped to 1.59. This could be due to the attainment of stoichiometry of boron and nitrogen with a consistent amount of carbon in the film (about 8%) and negligible oxygen.

4.4.4 On Film Stress

At lower flow ratios of 10:1 of NH_3:TEAB (Figure 4.9), the films were mildly tensile and the values are comparable (about 50MPa). With increase in the ammonia flow rate, the stresses in the film changed from mildly tensile to mildly compressive and the trend continued at higher flow ratios of 50:1 at 550°C. Within the temperature ranges studied the highest compressive stress attained was about 150 MPa. The effect is mainly due to the influence of ammonia which increases the nitrogen percentage in the films since the carbon percentage is almost constant over this range of temperature.

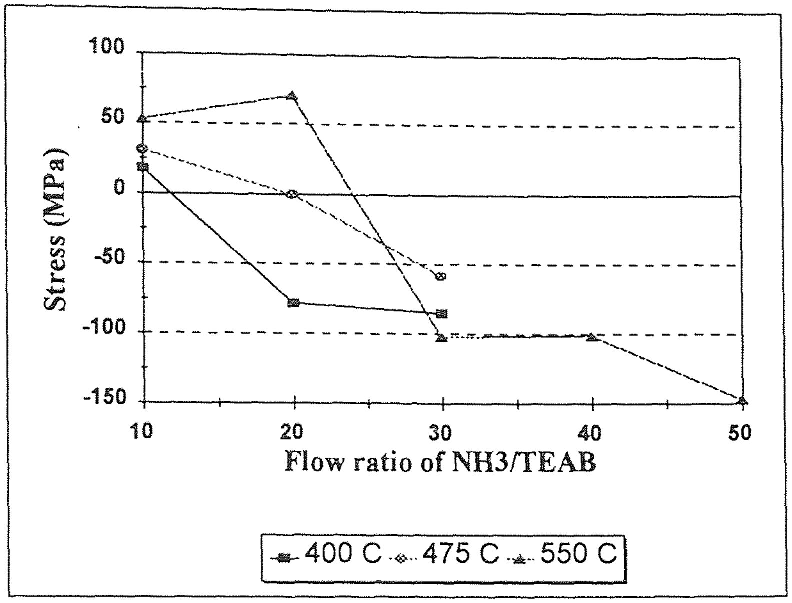

Figure 4.9 Variation of stress with increasing flow ratio of NH_3/TEAB

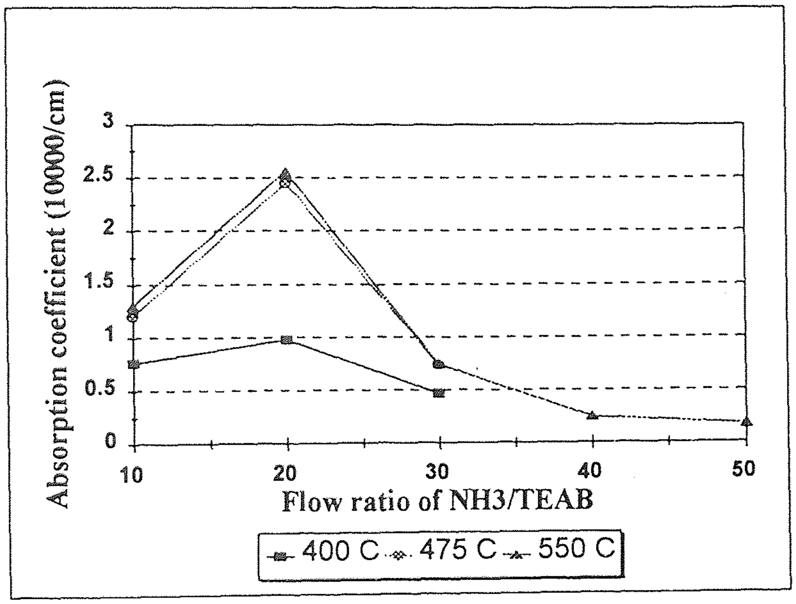

Figure 4.10 Variation of absorption coefficient with increasing flow ratio of NH_3/TEAB.

4.4.5 On Optical Transmission

Optical transmission measured using a UV/visible spectrophotometer is described earlier in this Chapter. The transmission was studied at a wavelength corresponding to red light ($\lambda = 6330Å$). The absorption coefficient α was calculated using Beer-Lambert law

$$I/I_o = \exp(-\alpha x)$$

where I/I_o is the fraction of the transmitted light and x, the thickness of the film.

All thickness' were normalized to 1 cm and the absorption coefficient was calculated. It can be seen from Figure 4.10 that the absorption coefficient shows a slight increase at 20:1 NH_3/TEAB flow ratio and subsequently drops to a low value of 0.18×10^4 cm^{-1} at 50:1 NH_3/TEAB flow ratio at 550°C. This indicates that near stoichiometric BN films are reasonably optically transparent.

4.5 Effect of Temperature

4.5.1 On Film Thickness

Figure 4.11 shows the variation of thickness of the film with increase in temperature. The thickness of the film constantly decreases with increase in temperature consistent with the growth kinetics as shown in Figure 3.2 [43]. The monotonic decrease in growth rate is due to the depletion of reactants caused by reactions on the hot walls at the front of the furnace. Evidence for that depletion is seen in the variation of thickness in the front and rear wafers of the back-to-back stress monitor Si wafers. The results is in agreement with the results of Adams et al.[12] for reactions involving diborane and ammonia where severe depletion effects were seen in the same temperature regime.

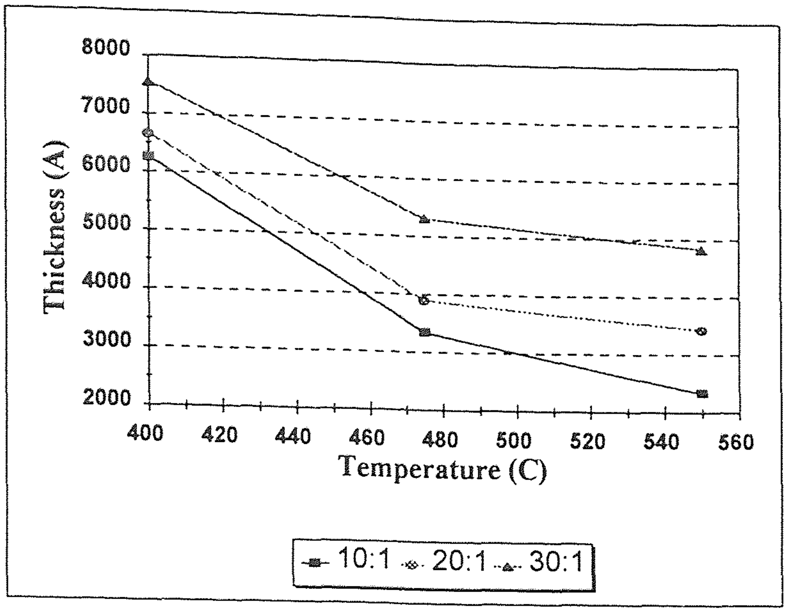

Figure 4.11 Variation of thickness with increasing temperature

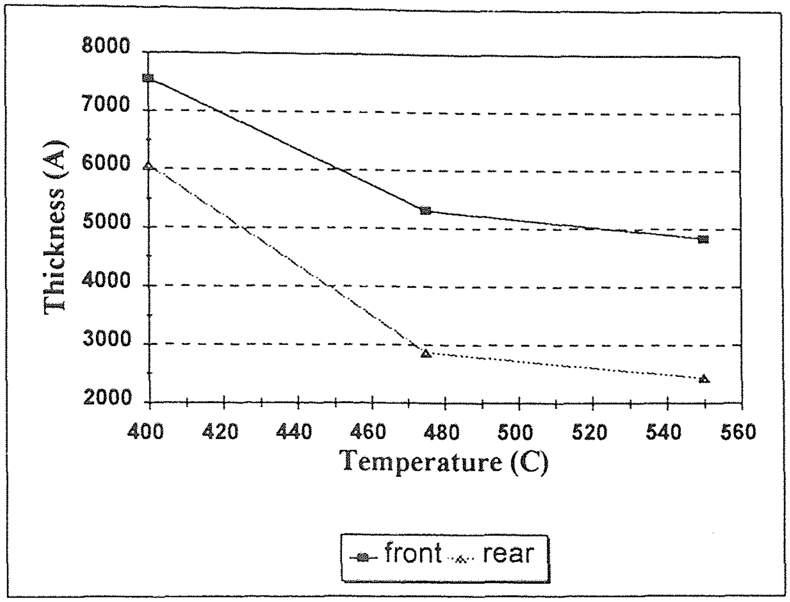

Figure 4.12 Effect of depletion on back-to-back stress monitors with increasing temperature at flow ratio of NH_3/TEAB of 10/1

Borane is generally considered to be the principal factor controlling the growth rate [12,29], its depletion with increase in temperature is reflected in both the growth rate as well as the film composition. Figure 4.12 shows the effect of depletion of the stress monitors with increase in temperature. At 400°C, the depletion is less but with increasing temperature the thickness of the wafer in front is almost double that of the one behind it. The depletion was more at higher temperatures (Figure 4.12). This is consistent with the results obtained by Levy et al. [45] showing depletion at temperatures of 550°C and less depletion at 400°C.

4.5.2 On Film Density

At lower flow ratios the films are denser and with a constant flow ratio of NH_3/TEAB = 10/1, with increase in temperature the films tend to become denser. But as the flow ratio of NH_3/TEAB is increased, the density decreases, probably resulting in porous films or as discussed earlier, the presence of carbon present in the films could have led to erroneous reading in the ellipsometer. In all, the density of films were comparable.

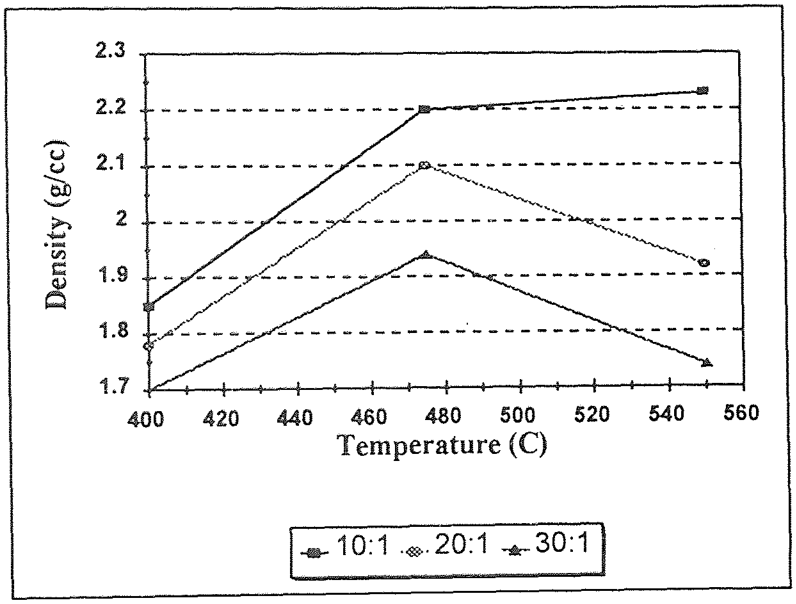

Figure 4.13 Variation of film density with increasing temperature

4.5.2 On Refractive Index

With increase in temperature the refractive index decreases (Figure 4.14) and this is consistent at the 3 temperatures studied. This is due to the tendency of the film towards stoichiometric boron nitride composition.

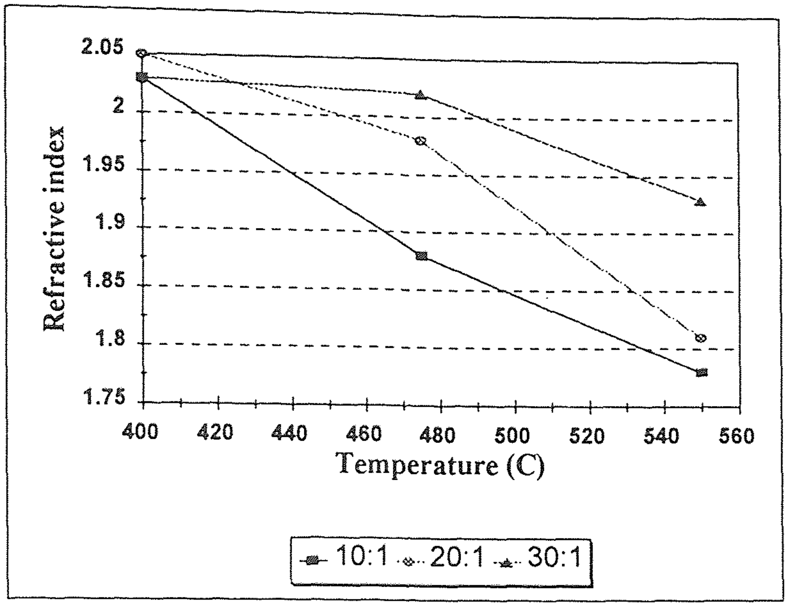

Figure 4.14 Variation of refractive index with increasing temperature

4.5.3 On Film Stress

At lower temperatures and low ammonia flow rate the films are mildly tensile (Figure 4.15) and the films become more tensile with increase in temperature. while at higher flow ratios and lower temperature, the films are mildly compressive and the compressive stress increases with increase in temperature. Interestingly, a transition from mildly compressive to mildly tensile behavior with increase in temperature was seen in the films at a constant NH_3/TEAB ratio of 20:1.

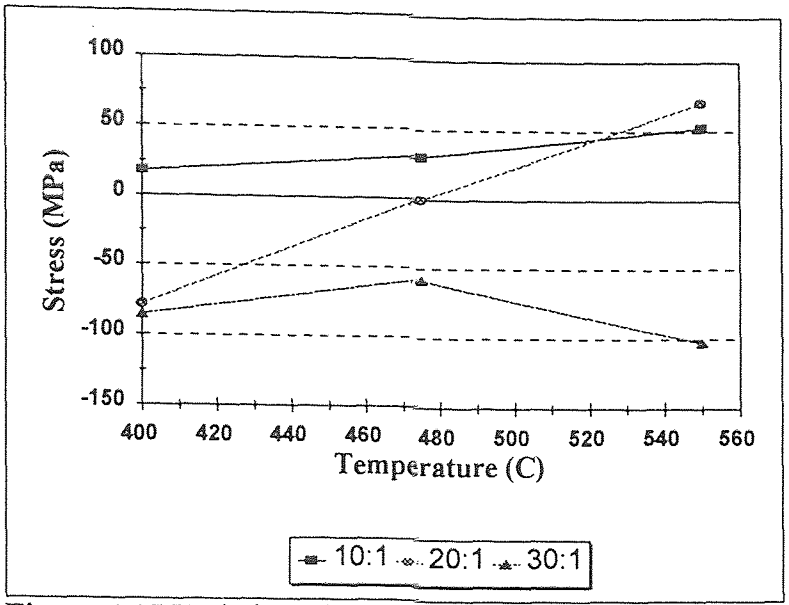

Figure 4.15 Variation of stress with increase in temperature

4.6 Electrical Characterization of BN Films

A detailed electrical characterization was done to determine the potentiality of the films as low ε IMD. Other than the dielectric constant measurement, leakage current and the trapped charge status were also measured. CV measurements was done for the films on both p-type and n-type Si substrates. Table 4.1 summarizes all the electrical data measured by I-V and C-V techniques.

Table 4.1 Electrical data measured for BN films

Substrate	Thickness (Å)	Dielectric constant	Fixed charge states/cm^2	Current at 0.5 MV/cm (nA/cm^2)	Resistivity (Ω-cm)
p-type Si	1400	3.2 - 3.5	-1.49 x 10^{12}	1.938	2.58 x 10^{14}
n-type Si	900	3.2 - 3.3	1.76 x 10^{12}	2.102	2.38 x 10^{14}

4.6.1 Dielectric Constant Measurements

The dielectric constant of BN films measured at least five locations on every sample showed in the range 2.7 to 4.8 with the resistivity more than 4 x 10^{14} Ω-cm. The breakdown voltage is more than 4 MV/cm which is the equipment limit. The dielectric constant is essentially constant from 100 Hz to 15 MHz measured in HP4194A. The dielectric constant ε was measured using the formula

$$\varepsilon = Cd/A$$

where d is the thickness of the film, A the area of the capacitor (area of the Al contacts - 300μm and 600μm) and C is the effective series capacitance of the dielectric as well as the intrinsic capacitance generated due the applied potential on the minority carriers of the dopant of the Si wafers. The latter varies with changes in applied voltage across the Al contacts.

Figure 4.16 shows the variation of dielectric constant of the films with increase in flow ratio at the three temperatures.

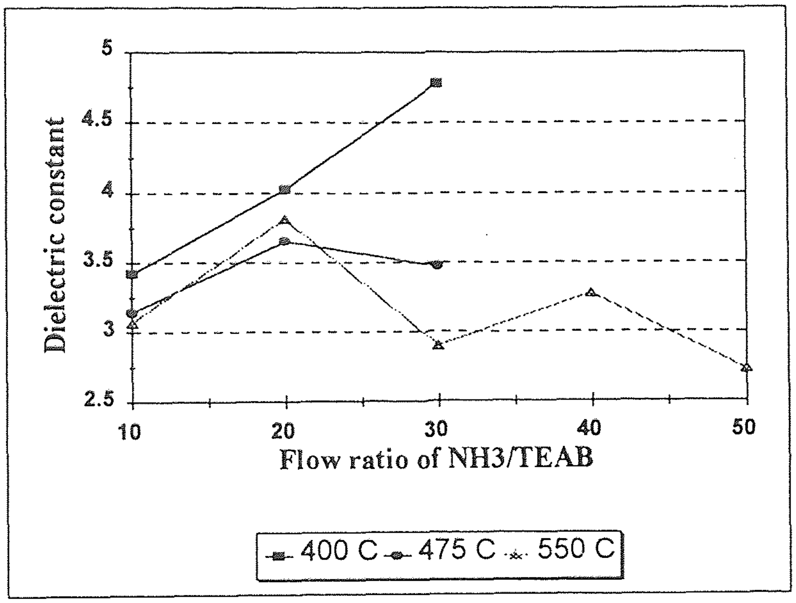

Figure 4.16 Variation of dielectric content with increasing flow ratio of NH_3/TEAB

It is seen that at lower temperatures the dielectric constant of the films increased with increase in flow ratio. This could be due to the varying stoichiometry in the films, or the variation of thickness of the film or could be due to the effect of carbon impurity in the boron nitride film. At the other 2 temperatures the dielectric constant showed a maximum at flow ratio of 20:1 and it decreased with increasing flow ratio. The least value obtained was 2.73 at a deposition of 550°C, pressure of 0.5 Torr and a flow ratio of NH_3/TEAB = 50/1. From the Auger analysis [45] also it is seen that the films tend to attain stoichiometry and more transparent films at these deposition conditions.

A dielectric constant reacts to electromagnetic radiation differently from free space because it contains electrical charges that can be displaced. For a sinusoidal electromagnetic wave, there is a change in the wave velocity and intensity described by the complex coefficient of refraction

$$n^* = n - ik$$

where n is the refractive index and k is the index of absorption. The coefficient of refraction is related to the complex dielectric constant $n^* = \varepsilon^* = \varepsilon' - i\varepsilon''$, where ε' is the relative dielectric constant and ε'', relative dielectric loss factor. Neglecting the imaginary terms, the dielectric constant (ε) is equal to the square of the index of refraction (n^2)

In Figure 4.17 the variation of dielectric constant, measured by the applied by the applied potential between the Al contacts (also known as static dielectric constant), and the optical dielectric constant (n^2) with increasing flow ratio at 400°C is shown. It is seen that there is a good correlation with the values of the 2 dielectric constants. A similar behavior is seen at the other two deposition temperatures. Thus by knowing the refractive index of the film, a fairly good idea of the dielectric constant of the material can be estimated.

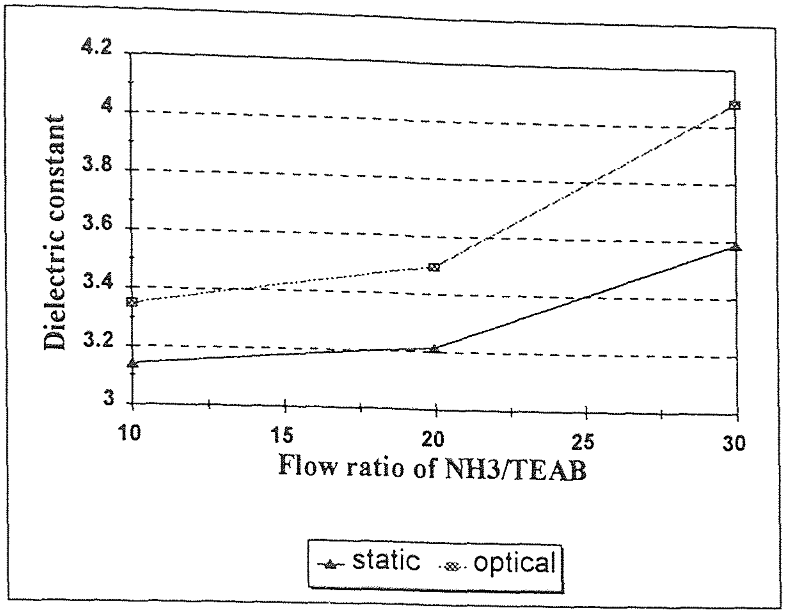

Figure 4.17 Comparison of the variation of static and optical dielectric constant with increasing flow ratio at 475°C

4.6.2 Current-Voltage (I-V) Characteristics of the Films

Figure 4.18 (a) and (b) shows the I-V characteristics of BN films deposited on p-type and n-type Si wafers respectively. Also, the variation of leakage current and resistivity of these dielectric films as a function of the flow ratio of NH_3/TEAB at deposition temperatures of 475°C and 550°C. The resistivity of the films was always greater 4.5 x 10^{14} Ω-cm. This is higher than the value obtained by other researchers [1,3,8,13] who deposited BN by CVD technique and is comparable to the value obtained by deposition of these films by plasma pulse method [25].

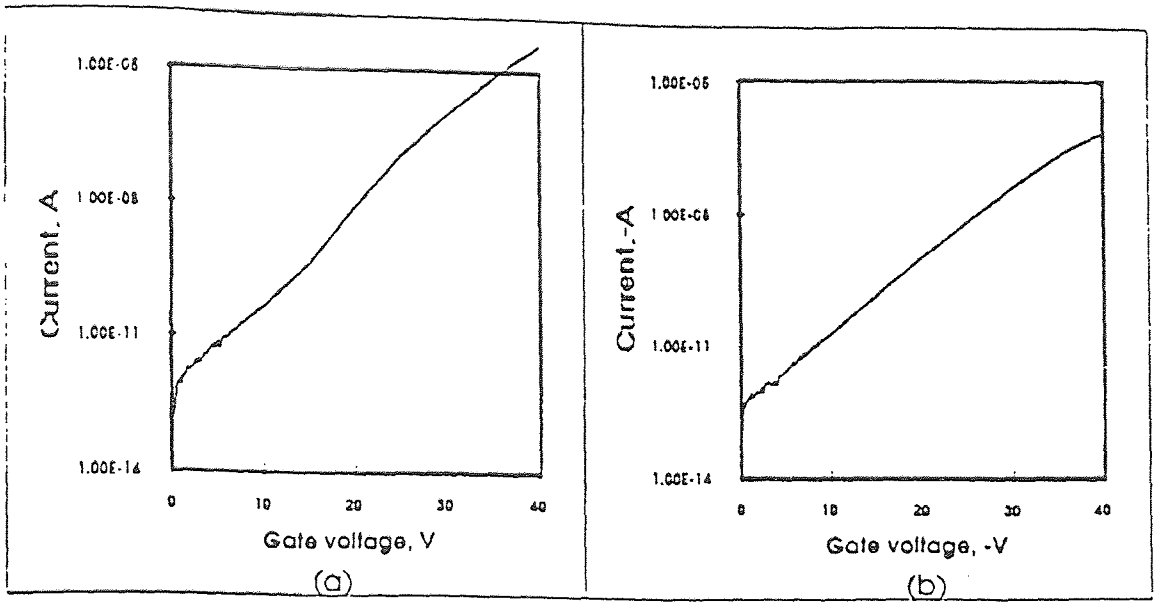

Figure 4.18 I- V characteristics of BN films on (a) n-type Si and (b) p-type Si

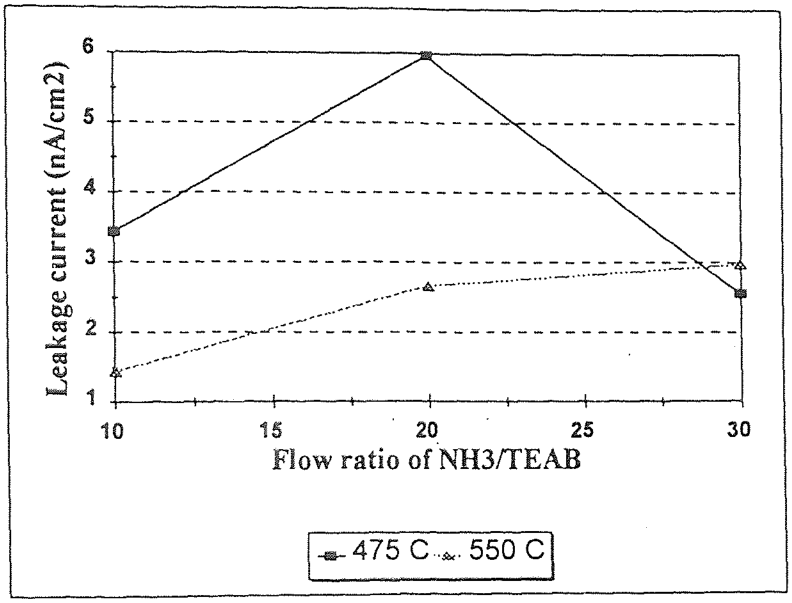

Figure 4.19(a) Variation of leakage current with increasing flow ratio of NH_3/TEAB at 475°C and 550°C at 0.5 MV/cm

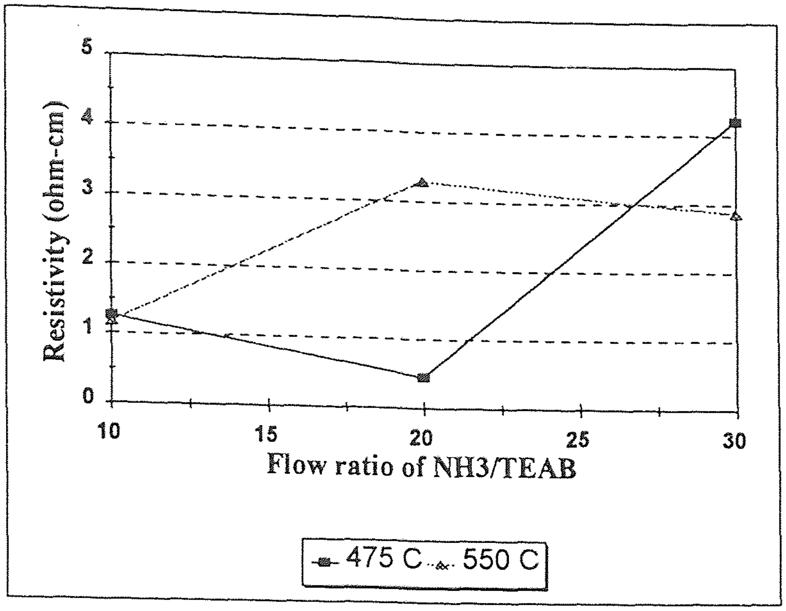

Figure 4.19(b) Variation of resistivity with increasing flow ratio of NH_3/TEAB at 475°C and 550°C at 0.5 MV/cm

4.6.3 Bias-Temperature Stress Study of BN Films

The mobile charge and trap state densities are inferred in the work by the measured C-V flat-band shift shown in Figure 4.20 (a) and (b) for annealed and unannealed contacts corresponds to some kind of charge states either in the interface or in the bulk of the insulator. Though some of the charges was passivated by forming gas anneal, there was still a big flat-band voltage shift. Thus several tests were done to identify the origin of the charges in the C-V shift.

In the next step, a bias stress study was made. A bias of ± 1 MV/cm were applied for 2-5 minutes at room temperature. C-V measurement was done after each polarity of stress. Figure 4.21 (a) and (b) illustrates these results.

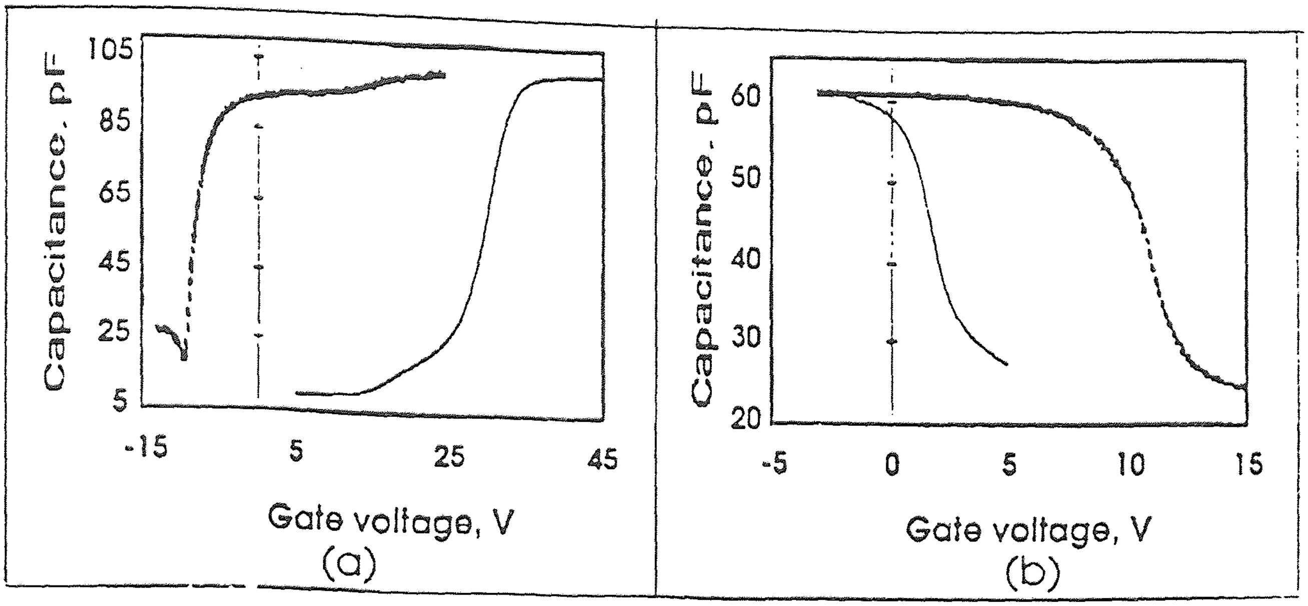

Figure 4.20 C-V characteristics before and after contact annealing on (a) n-type Si and (b) p-type Si. Solid line is before and dotted line after contact annealing

The flat-band voltage shift indicates that in addition to mobile ions, there is trapped positive charges in the bulk of the insulator. To confirm the above findings, a bias-temperature stress on these BN samples. A ± 0.5 MV/cm field is applied for 10 minutes at 120°C for both n-type and p-type substrates. The results are as shown in Figure 4.22 (a) and (b). This is also in confirmation of the findings in Figure 4.21. To determine the nature of the trapped charges, a bias-temperature aging where the samples were under field stress for 10 minutes at 120°C. A field of 1 MV/cm is applied for 10 minutes, C-V is measured, and the reverse field of -1 MV/cm is applied for the same time and the C-V is measured. This process is repeated again after the last measurement. The result is illustrated in Figure 4.23 (a) and (b). The flat band voltages for the above measurements are tabulated in Table 4.2.

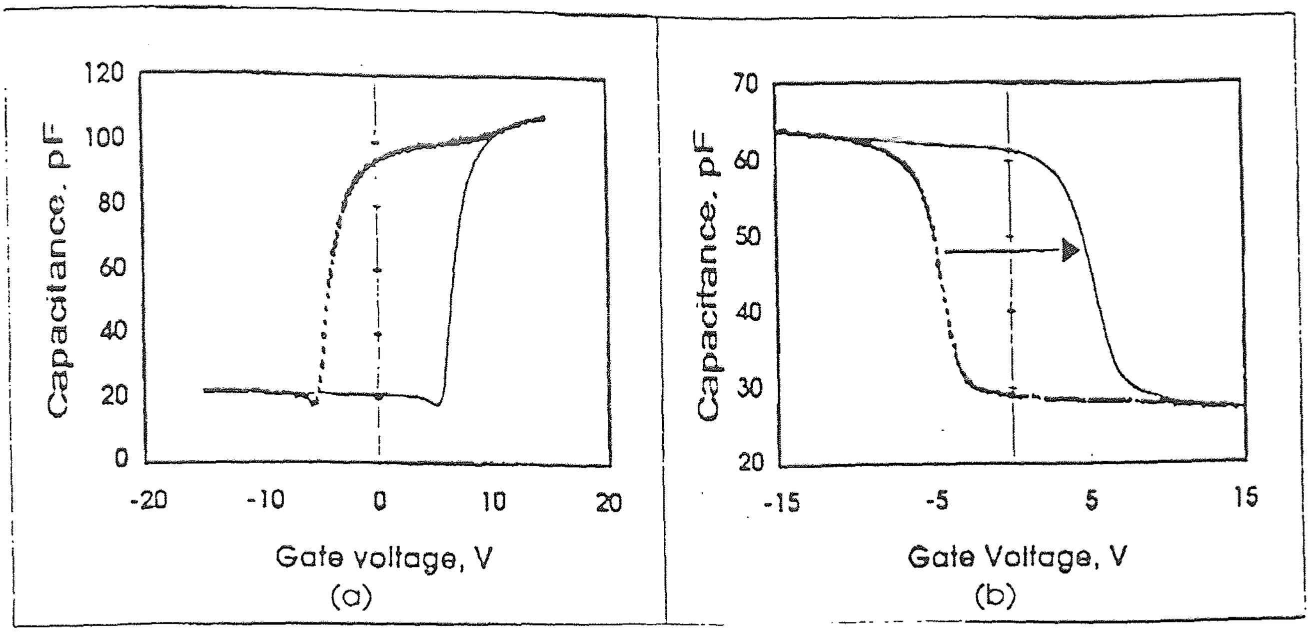

Figure 4.21 C-V characteristics under negative and positive field stress for (a) n-type Si and (b) p-type Si. Solid line is for positive stress, dotted for negative stress

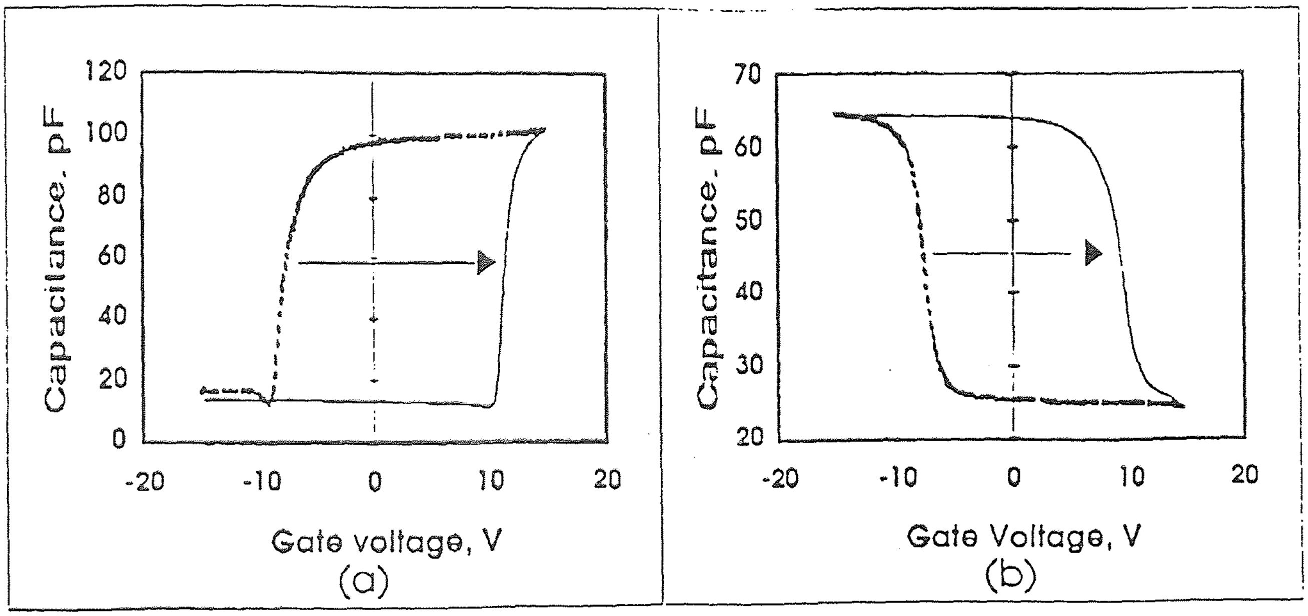

Figure 4.22 C-V characteristics under negative and positive field stress at 120°C for (a) n-type Si and (b) p-type Si. Solid line for positive stress, dotted for negative stress

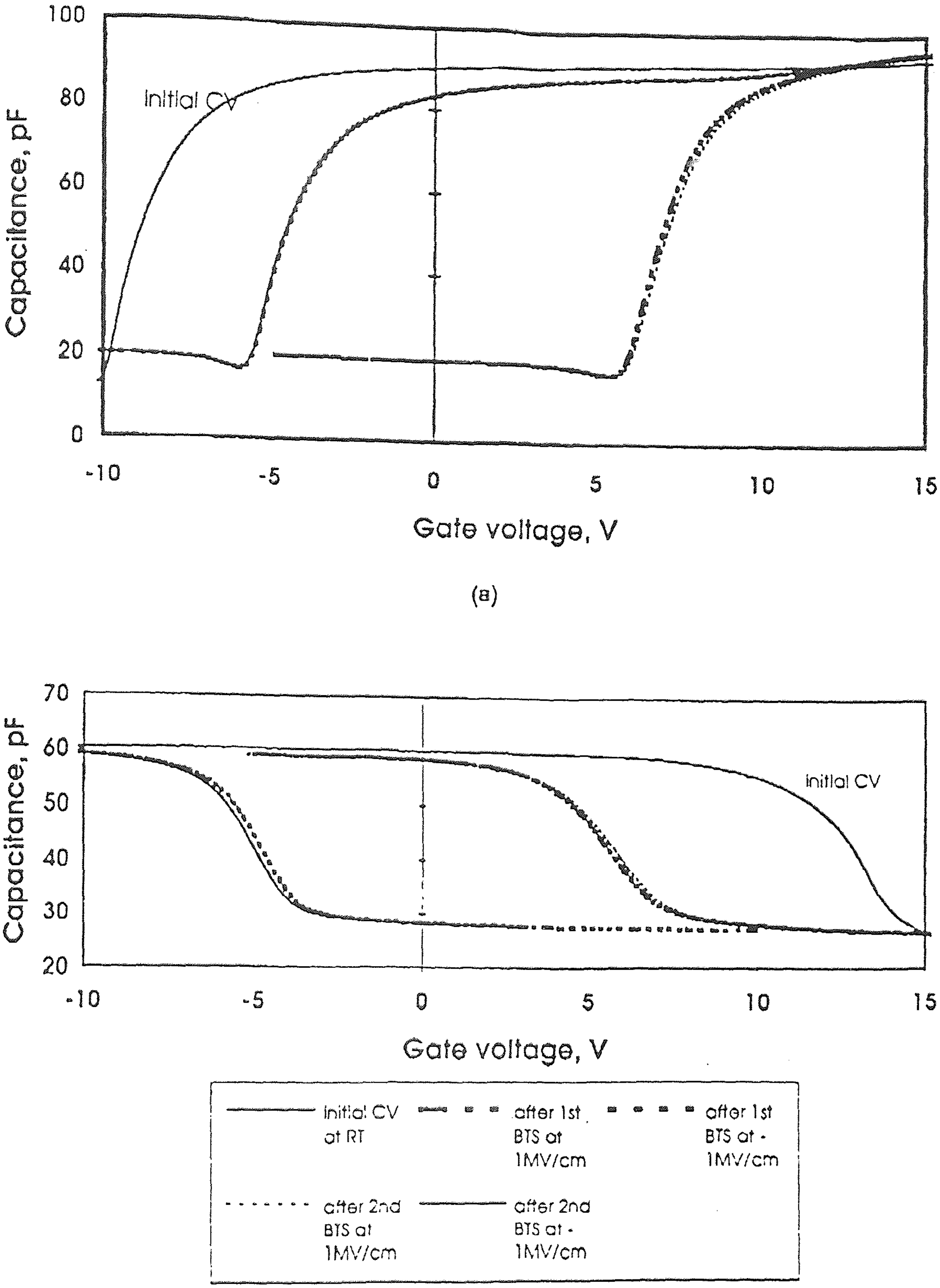

(a)

(b)

Figure 4.23 C-V characteristics under negative and positive field stress cycle at 120°C for (a) n-type and (b) p-type

Table 4.2 Flat-band voltage under different bias-temperature stress

Type of Si	**Nature of stress**	**V_{fb} (V)**
	Effect of field stress	
p-type	after -1 MV/cm bias for 2 minutes	- 7.960
p-type	after 1 MV/cm bias for 2 minutes	+9.234
n-type	after -1 MV/cm bias for 2 minutes	- 8.330
n-type	after 1 MV/cm bias for 2 minutes	+11.080
	Effect of bias-temperature stress	
p-type	after -0.5 MV/cm for 10 minutes at 120°C	- 5.306
p-type	after 0.5 MV/cm for 10 minutes at 120°C	+4.577
n-type	after 0.5 MV/cm for 10 minutes at 120°C	+6.654
n-type	after -0.5 MV/cm for 10 minutes at 120°C	- 4.230
	Effect of bias-temperature stress cycle	
p-type	Room temperature CV	+11.880
p-type	after -1 MV/cm for 10 minutes at 120°C	- 5.747
p-type	after 1 MV/cm for 10 minutes at 120°C	+5.040
p-type	after -1 MV/cm for 10 minutes at 120°C	- 5.934
p-type	after 1 MV/cm for 10 minutes at 120°C	+4.665
n-type	Room temperature CV	-7.646
n-type	after 1 MV/cm for 10 minutes at 120°C	+6.797
n-type	after -1 MV/cm for 10 minutes at 120°C	- 4.230
n-type	after 1 MV/cm for 10 minutes at 120°C	+7.261
n-type	after -1 MV/cm for 10 minutes at 120°C	- 4.270

From Figure 4.23 and Table 4.2, it is evident that the flat-band never went back to its original value for both p-type and n-type Si substrates. Bias temperature cycle thus not only indicates the presence of mobile ions, it also shows the presence of trapped positive charges in the bulk of the insulator. Although some of the trapped negative charges can be discharged in the gate or in the semiconductor, the trapped positive charges are essentially immobile on this field and temperature range. These trapped charges could be due to the dangling bonds caused by the following 2 reasons:

1. the boron rich nature of this non-stoichiometry of the films
2. the elemental carbon in the films.

These two facts is already shown in the Auger analysis. Low precursor ratio yielded boron rich films whereas high substrate temperatures caused the unbonded excessive carbon.

The flat-band voltage shift is shown in Table 4.3. Other than electron trapping (n-type) or hole trapping (p-type) in the insulator, there is also an indication of having mobile charge in the interface. Figure 4.24 (a) and (b) illustrates the BTS cycles for an n-type and p-type deposited at 475°C and 550°C respectively at an NH_3/TEAB flow ratio of 10/1.

Table 4.3 Flat-band voltage under different bias-temperature stress

Deposition condition	Type of Si	Nature of stress	V_{fb}, V
		Effect of BTS cycle	
475°C 0.5 Torr NH_3/TEAB = 10/1	n-type	Room temperature C-V	2.66
	n-type	after +1 MV/cm for 10 min. At 120°C	5.04
	n-type	after -1 MV/cm for 10 min. At 120°C	1.205
	n-type	after +1 MV/cm for 10 min. At 120°C	5.7
	n-type	after -1 MV/cm for 10 min. At 120°C	1.465
550°C 0.5 Torr NH_3/TEAB = 10/1	p-type	Room temperature C-V	6.5
	p-type	after -1 MV/cm for 10 min. At 120°C	-4.54
	p-type	after +1 MV/cm for 10 min. At 120°C	4.92
	p-type	after -1 MV/cm for 10 min. At 120°C	-4.99
	p-type	after +1 MV/cm for 10 min. At 120°C	4.05
550°C 0.5 Torr NH_3/TEAB = 30/1	p-type	Room temperature C-V	6.78
	p-type	after -1 MV/cm for 10 min. At 120°C	7.98
	p-type	after +1 MV/cm for 10 min. At 120°C	5.39
	p-type	after -1 MV/cm for 10 min. At 120°C	8.19
	p-type	after +1 MV/cm for 10 min. At 120°C	5.93

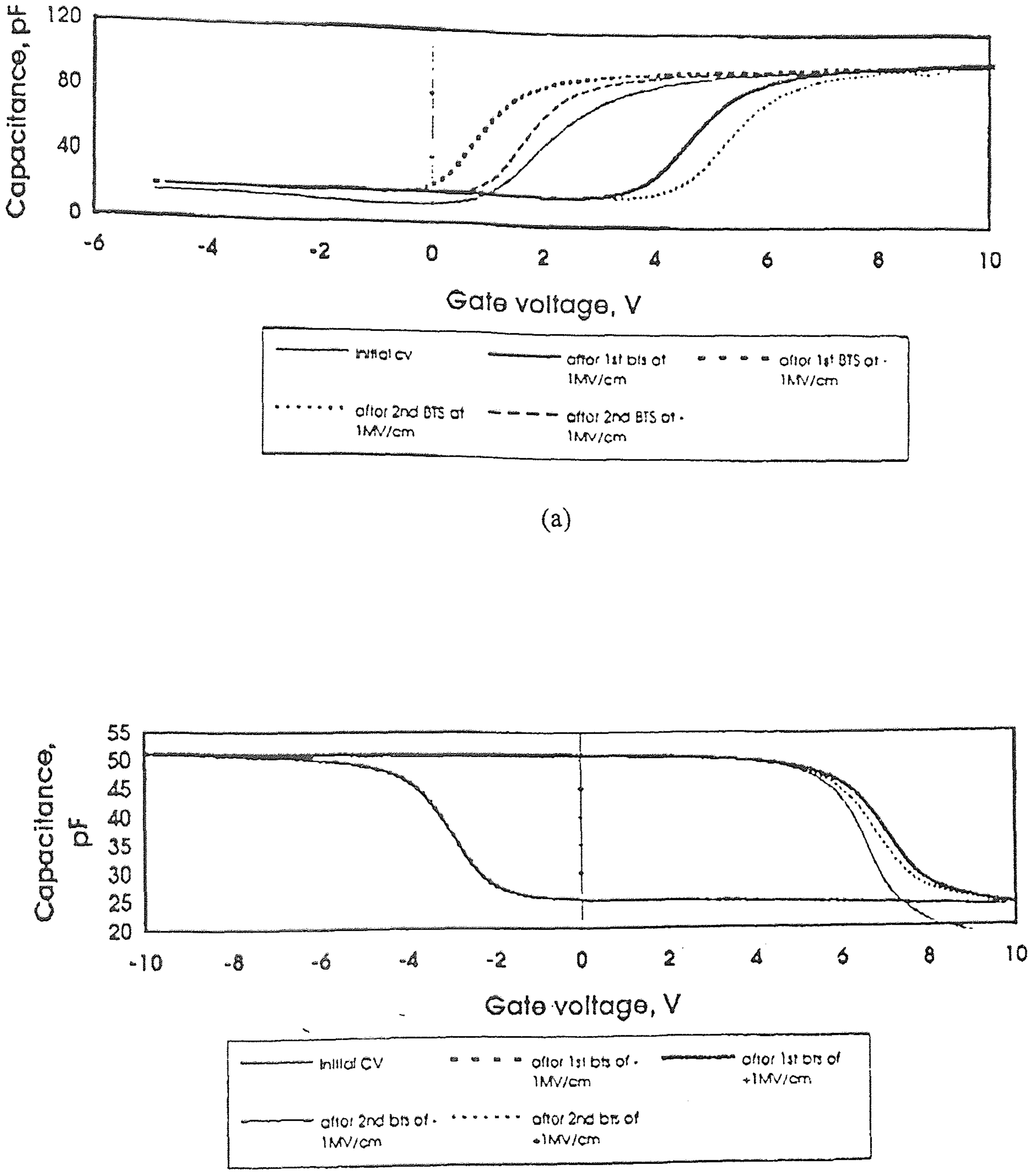

(a)

(b)

Figure 4.24 BTS cycle stress of BN films on (a) n-type Si and (b) p-type Si

Thus there are several facts revealed from this study. First, forming gas contact annealing passivates some of the charges caused by metal evaporation. Second, CV shift in response to the polarities indicates a presence of mobile ions in the insulator. Third, there is considerable trapped immobile charges in the bulk of the insulator for which the flat-band does not go back to the original value prior to the aging. Fourth, the possibility of trapped negative charges being attracted to the gate electrode or to the semiconductor and consequently being discharged cannot be excluded.

CHAPTER 5

CONCLUSIONS

Boron nitride thins films processed in this study were amorphous, uniform and they were boron rich at lower temperatures, but with increasing temperature, the films attained compositions close to stoichiometric BN. There was about 8% carbon in the films which was not in a compound form. This made the refractive index measurements difficult. It was found that the stress on the films were either mildly tensile or compressive (+100MPa - -150MPa) depending on the deposition conditions. The static dielectric content varied from 4.78 to 2.73 depending on the deposition condition. The optical and the static dielectric constant behavior were similar. At higher flow rates the films tend to be stoichiometric and transparent. The presence of mobile charge carriers in the films as well as at the substrate-film interface could be a reason for the dielectric constant limitation of a value of about 2.7. However this a reduction of about 33% of the average reported value of four.

Thickness should be measured by some other techniques, probably by Tencor/SEM. The carbon concentration measurement could be interesting. A stoichiometric film with lower C content could possibly give lower dielectric constant films. Further study can be gone by adding small amounts of Si into the film to improve its stability. The hygroscopic nature of stoichiometric BN and its effect on dielectric properties could be studied.

BIBLIOGRAPHY

1. M.J. Rand and J.F. Roberts, J. Electrochem. Soc., **15**, 423 (1968).
2. S.P. Murarka, C.C. Chang, D.N.K. Wang and T.E. Smith, J. Electrochem.Soc., **126**, 1951 (1979).
3. M. Hirayama and K. Shohno, J. Electrochem. Soc., **122**,1671 (1975).
4. W. Baronian, Mat. Res. Bull., 7,119 (1972).
5. M Sano, Thin Solid Films, **83**, 247 (1981).
6. S Motojima, Y. Tamura and A. Sugiyama, Thin Solid Films, **88**, 269 (1982).
7. T. Takahashi, H. Itoh and A. Takeuchi, J. Crystal Growth, **47**, 245 (1979).
8. T. Takahashi, H. Itoh and M. Kuroda, J. Crystal Growth, **53**,1981 (1981).
9. K. Nakamura, J. Electrochem. Soc.,**132**, 1757 (1985).
10. S.S. Dana and J.R. Maldonado, J. Vac. Sci. Technol., **B4**, 235 (1986).
11. A. C. Adams, J. Electrochem. Soc., **128**, 1378 (1981).
12. A. C. Adams and C.D. Capio, J. Electrochem. Soc., **127**, 399 (1980).
13. S.B. Hyber and T.O. Yep, J. Electrochem. Soc., **123**, 1721 (1976).
14. O. Gafri, A. Grill and D. Itzhak, Thin Solid Films, **72**,523 (1980).
15. W. Schomolla and H.L. Hartnagel, J. Appl. Phys., **15**,L95 (1982).
16. W. Schomolla and H.L. Hartnagel, Solid State Electronics, **26**, 931 (1983).
17. A.J. Noreika, and M.H. Francombe, Thin Solid Films, **101**, 722 (1983).
18. M.D. Wiggins and C.R. Aita, J. Vac. Sci. Technol. **A2**, 322 (1984).
19. E.H. Lee and H. Poppa, J. Vac. Sci. Technol., **14**, 223 (1977).
20. C. Weissmantel, K. Bewilogua, K. Breuer, D. Dietrich, U. Ebersbach, H.J. Erler, V. Rao and G. Reisse, Thin Solid Films, **96**, 31 (1982).

21. C. Weissmantel, J. Vac. Sci. Technol., **18**, 2082 (1981).

22. S. Shanfield and R. Wolfson, J. Vac. Sci. Technol., **A1**, 323 (1983).

23. M. Satou and F. Fujimoto, J. Appl. Phys., **22**, L171 (1983).

24. L. Guzman, F. Marchetti, I. Scotoni and F. Ferrari, Thin Solid Films, **117**, L63 (1984).

25. M. Sokolowski, A. Sokolowska, A. Michlski, Z. Romanowski, A.R. Mazurek and M.Wronikowski, Thin Solid Films, **80**, 249 (1981).

26. W.A. Johnson, R.A. Levy, D.J. Resnic, T.E. Saunders, A.W. Yanof, H. Oertel, H. Huber, and , J. Vac. Sci. Technol. **B5**, 257 (1987).

27. R.A. Levy, D.J. Resnic, R.C. Frye, A.W. Yanof, G.M. Wells and F. Cerina, J. Vac. Sci. Technol., **B6**, 154 (1988).

28. D. Maydan, G.A. Coquin, H.J. Levinstein, A.K. Sinha, and D.N.K. Wang, J. Vac. Sci. Technol. **16**, 1959 (1979).

29. R.E. Acosta, J.R. Maldonado and R. Fair, J. Vac. Sci. Technol. **B4**, 240 (1986).

30. R.K.Laxman, Semicond. Int., **5**, 71 (1995).

31. T. Usami, K. Shimokawa and M. Yoshimaru, J. Appl. Phys., **33**, 408 (1994).

32. M. Hatanaka, Y. Mizushima, O. Hataishi and Y. Furumura, Proc. VLSI Multilevel Interconnection Conf., 435 (1991).

33. B.L. Chin and E.P. Van de Ven, Solid state Technol., **31**, 119 (1988).

34. D. Yu, D. Favreau, E. Martin and A. Manocha, Proc. VLSI Multilevel Interconnection Conf., 166 (1990).

35. S. Mizuno, A. Verma, P. Lee and B. Nguyen, Int. Conf. On Metallurgical Coatings and Thin Films Abstract (1995)

36. D.C. Rich, P. Cebe and A.K. St.Clair, Mat. Res. Soc. Symp. Proc. **323**, 301 (1994).

37. Y. Negi, Y. Suzuki, I. Kawamura, T. Hagiwara, Y. Takahashi, M. Ijima, Y. Imai and M. Kakimoto, J. Polym. Sci. **A30**, 2281 (1992).

38. M. Maeda, Japan. J. Appl. Phys., **29** 1789 (1990).

39. M. Maeda, T. Makino, E. Yamamoto and S. Konaka, IEEE Trans. Electron Devices, **36**, 1610 (1989).

40. M. Maeda and T. Makino, Japan. J. Appl. Phys., **26**, 660 (1987).

41. S.V. Nguyen, A. Nguyen, H. Treichel and O. Spindler, J. Electrochem. Soc., **141**, 1635 (1994).

42. V. Paturi, "Synthesis and Characterization of BN Thin Films for X-ray Masks", MS Thesis, New Jersey Institute of Technology, Newark, NJ (1991).

43. W.P. Kuo, "Synthesis and Characterization of LPCVD Boron Nitride Films for X-ray Lithography, MS Thesis, New Jersey Institute of Technology, Newark, NJ (1993).

44. Advanced Semiconductor Materials America, Inc., "Micro 3 Manual".

45. R.A. Levy, E. Mastromatteo, J.M. Grow, V. Paturi and W.P. Kuo, J. Of Mater. Res., **10**, 320 (1995).

46. R.A. Levy, Microelectronic Materials and Processes, Kluwer Academic Publishers, 1989.